INSTITUTE OF HYDROLOGY

Report No. 31

April 1976

A NON-LINEAR URBAN RUNOFF MODEL

by

C H R Kidd

ABSTRACT

One of the prime requisites for the efficient design of flow capacities of storm water sewerage systems is the ability to simulate mathematically the physical phenomena of the urban runoff process. The purpose of this study is to investigate the above-ground phase of the urban runoff process, and a lumped-parameter nonlinear model is postulated for its simulation, in addition to two simpler models (linear and time of entry) for the purposes of comparison. Two models of differing complexity for the simulation of the below-ground phase are also postulated.

Two small catchments (.6 and .8 ha) in the Lordshill area of Southampton have been monitored continuously for rainfall and runoff since June 1974, and suitable storm events reduced to a condition suitable for analysis. It is considered that the two catchments are of small enough size that the performance of the above-ground model should not be obscured by possible inaccuracies of the below-ground model.

The model performance is demonstrated with the monitored rainfall as input, and the modelled and observed outfall hydrographs compared for 19 storm events on the two catchments. It is concluded that the nonlinear surface routing submodel provides a better synthesis of the above-ground phenomena than the linear or time of entry submodels.

CONTENTS

FIGURES

INTRODUCTION

As enormous expense is involved in the construction of urban storm drainage systems, any improvements to the design methods for the efficient determination of optimum sewer size and artificial storages are very welcome. This report is concerned with the mathematical conversion of rainfall to runoff, an essential part of all design methods; it does not cover the equally important economic or statistical probability aspects of design problems.

Before an urban runoff model may be used in a design method, it must undergo two stages of development. The first stage is construction and validation, which involves the postulation of the model mechanics and a demonstration that the model provides a valid description of the physical phenomena, best achieved by the attempted reproduction of observed runoff from observed rainfall input. The second stage is the calibration of the model, and is necessary where model parameters cannot be estimated directly from physical considerations. It is likely that the calibration would take the form of a statistical regression, using a quantity of data, relating the unknown parameters to catchment characteristics. This study is concerned only with the first of these two stages, and postulates a particular model with a demonstration of its validity.

The urban runoff process may be seen as a two-phase phenomenon, incorporating an above-ground phase and a below-ground phase. Unfortunately, there is no conveniently clearcut interface between the two phases. For the purposes of this study, the above-ground phase is seen as the conversion of the rainfall falling on a given subcatchment into the runoff contribution at a manhole in the sewer system, where this manhole is considered as the collection point for the given subcatchment. As such, this phase incorporates not only such elements as surface routing but also the routing of flows connecting gullies with the manhole or junction in the sewer system. The below-ground phase of the urban runoff process is concerned with the combining and routing of the inlet hydrographs through the sewer system to the outfall. It would seem likely that any improvement in design models will arise out of a separate treatment of the two phases - the first essentially hydrological and the second more of a hydraulic process. The urban runoff data existing in this country generally relate to relatively large catchments where the behaviour of the model of the one phase becomes obscured by the behaviour of the other. In this manner it is not possible to say whether a right answer has been achieved by a product of two correct or two incorrect simulations.

The urban runoff phenomenon on catchments of sufficiently small size was investigated so that the effects of the deficiencies of the below-ground model should be negligible in comparison with those of the above-ground model. A better understanding of the above-ground phase was thus possible, and a submodel for this phase was developed which may be assumed to produce a realistic synthesis of the above-ground behaviour. It had been the intention to collect data at the phase boundary in order to eliminate the need for modelling the below-ground phase at all.

However, it was found impracticable to develop suitable instrumentation for such an exercise and thus the monitoring of the two catchments used in this study may be seen as a compromise. It is considered that the sewer system is still of a sufficiently small size for the above-ground phase to be the predominant part of the whole process. Thus, while it is necessary to postulate a below-ground model, it was not the purpose of this study to investigate the relative merits of different below-ground models.

I: THE ABOVE-GROUND MODEL

The catchment is divided into subcatchments, each of which contribute to an individual junction of the sewer system. In the sense used in this study, the words "junction" and "inlet" are synonymous and refer to the subcatchment collection point. This is not to be confused with a gully-trap, any number of which may contribute to a given inlet. In general, the word "inlet" is used when considering the above-ground phase, and the word "junction" used for the below-ground phase, and the point at which either occur is the phase boundary. The model is concerned with the conversion of the rainfall hyetograph into the inlet hydrograph.

The model recognises any number of different surface types, each of which will operate on the rainfall hyetograph in different ways depending on the physical characteristics of the particular surface. The two contributing types considered in this study are paved surfaces (roads, paths, driveways, car parks) and roofed surfaces. It is thus assumed that the contribution from pervious surfaces may be ignored.

The justification of the latter statement lies in the generally low values of percentage runoff found for catchments in this country. The Road Research Laboratory data (1962) of the 1950s indicated that values of percentage runoff from impervious surfaces only were consistently less than 100%. The traditional methodology in this country has been to accept 100% runoff from impervious areas and none from pervious areas. Both assumptions are to some extent incorrect, but it is true to say that the errors incurred in the two assumptions do have a tendency to cancel each other out. However, it would appear from the RRL data mentioned above that the assumption of 100% runoff from impervious areas is more in error than the other, and this tendency is supported by the data employed in this study. It is felt that the contribution from pervious areas, while affecting the volume of runoff, has little effect on the mechanics of the conversion from rainfall hyetograph to inlet hydrograph. The assumption that the pervious areas may be neglected is one which is based on experience in this country only. In other countries, where higher rainfall intensities are experienced, values of percentage runoff from impervious surfaces are found to be well in excess of 100%, and such an assumption may not be justified in such circumstances.

The conversion of rainfall hyetograph to inlet hydrograph is achieved by the use of three submodels, the Depression Storage Submodel, the Percentage Runoff Submodel and the Surface Runoff Submodel.

Depression storage submodel

The depression storage is that part of the rainfall which is retained on the surface of the ground and thus never reaches the inlet and the sewer system. It may be seen as a function of two components: that layer of water which is held to the ground surface by surface tension, or initial wetting, and that water which is held in puddles where the configuration of the ground surface does not allow the water to flow to the inlet. These two components are best treated together, and the depression storage conceived as a depth of water spread evenly over the catchment.

The assumption is made that the depression storage must be satisfied before any runoff may occur. This assumption is not strictly realistic, since it is clear that some runoff could occur from ground close to a road gully before puddles in other parts of the subcatchment are completely filled. However, it is considered that the simplicity of

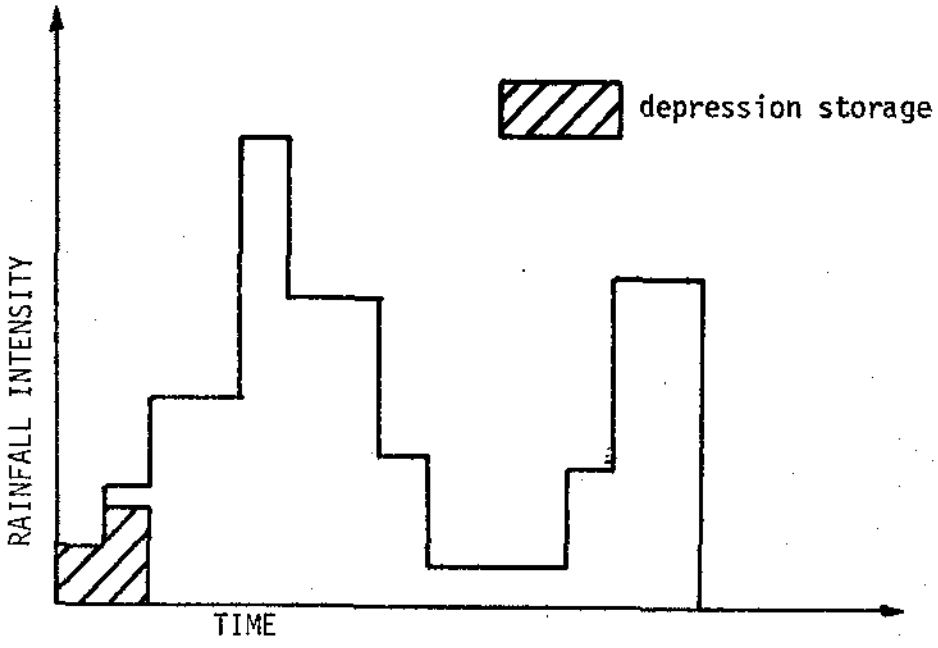

Figure 1: The application of the depression storage submodel.

such an assumption justifies its use, since the precise nature of its temporal distribution is unknown and would vary greatly from one subcatchment to another and perhaps even from storm to storm. Furthermore, it is felt that such an assumption is likely to have a small enough effect on the model output to be justified. The application of the depression storage submodel is demonstrated in Figure 1. The value of the depression storage is taken to be constant for a given catchment, the submodel thus having one parameter for each surface type.

The percentage runoff submodel

As has been noted above, the volume of rainfall falling on the paved surfaces after depression storage is not the same as the volume of runoff. Thus some adjustment is required to the rainfall hyetograph, such that the rainfall and runoff volumes are the same. This adjustment needs to be looked at in two ways, depending upon whether the percentage runoff is greater or less than 100%. The percentage is obtained from the ratio of rainfall volume falling on the impervious surfaces to runoff volume.

If the percentage runoff is less than 100%, then the difference may be seen as rainfall "loss", in the same way as infiltration (there is little doubt that some of the water does in fact infiltrate). The loss is assumed to be constant throughout the duration of rainfall, as is illustrated in Figure 2. This is in effect a traditional ∅-index model. The rainfall hyetograph is in this manner converted into a net rainfall hyetograph.

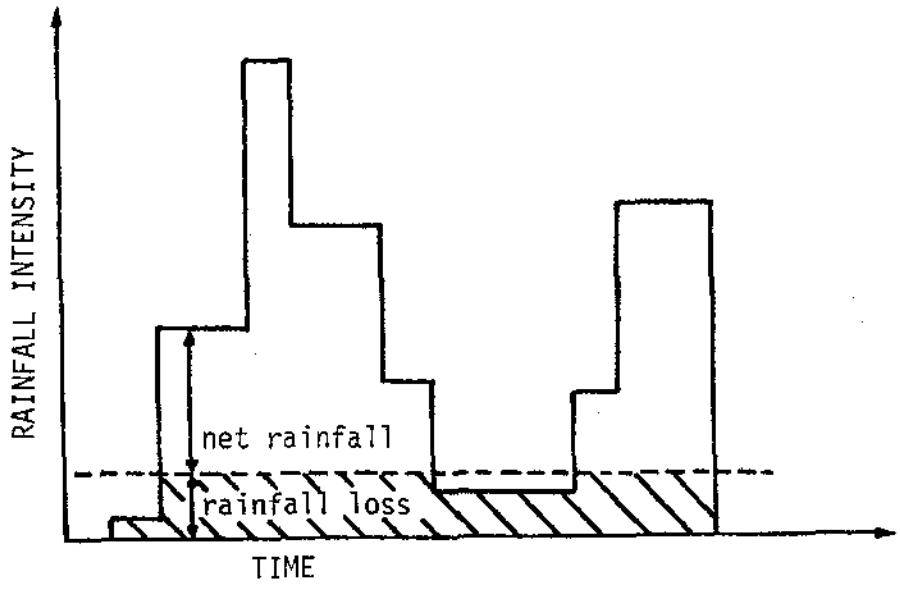

Figure 2: The application of the percentage runoff submodel (for percentage runoff less than 100).

In circumstances where the percentage runoff is greater than 100%, then the contributing area (paved) is multiplied by a value such that the rainfall and runoff volumes are equal. It would be possible to add a constant value of rainfall, analogous but opposite to the previous case, but this cannot be explained physically. In fact, it makes no difference to the overall model in the case of the linear surface routing submodel (next section), but it would affect the nonlinear surface routing submodel where the nature of the response depends upon size of the input. It is fair to say that neither of the above methods is completely realistic, as they correspond directly to the impervious/

pervious assumptions mentioned earlier.

The percentage runoff submodel is applied only to the paved surfaces, because it is felt that this is where the inconsistencies between rainfall and runoff volumes are likely to occur. It is also true that any contribution from pervious surfaces will reach the inlet by way of the paved surfaces. All rainfall falling on to the roofs, after depression storage is satisfied, is taken to contribute.

Surface routing submodel

The surface routing submodel is concerned with routing the excess rainfall over the surfaces and into the inlet. In the case of the paved surfaces, this includes such elements as overland flow, gutter flow, and flow through gully traps and through the short length of pipe connecting the trap to the sewer system. In the case of roofed surfaces, this is over-roof flow, and flow along gutters, down down-pipes and through the length of pipe connecting the downpipes to the sewer system.

The deterministic approach: It can be seen that the surface routing part of the urban runoff process is a combination of a number of complex contributary processes. As such this phase does not lend itself well to a deterministic solution for the following three main reasons.

The first objection is on the grounds of realism. A deterministic solution is one which attempts to describe mathematically the specific mechanical processes involved in any problem. This is not to say that such a solution does not make certain simplifying assumptions and generalisations along the way (for instance, the full St. Venant "shallow water" equations are themselves a product of several simplifications). Let us consider what is arguably the predominant feature of the above-ground phase, the overland flow phenomenon. The most widely-used deterministic approach to the aspect, the kinematic wave model, was first postulated by Wooding (1965), and used extensively by Liggett and Woolhiser (1967), Carlos Bravo (1970), amongst others. This model assumes uniform sheets of water travelling across uniform planes, a concept which is not strictly realistic. As anybody who has observed overland flow will vouch, the water depth is non-uniform, with the process quickly degenerating into a complex configuration of discrete rivulets. Under heavy rainfall the flow regime is best described as chaotic. In the light of this, such a deterministic approach would appear to be little short of a highly complex conceptual model. The above argument says nothing of the effectiveness of the model, and, to its credit, its deterministic basis means that all parameters employed in the model are directly related to the physical characteristics of the catchment.

The other two objections are of a more practical nature, and are based on the assumption that such a model shall be used as a design tool. A deterministic model such as the kinematic wave model would require a highly complex description of the catchment. Firstly, this would

require an immense quantity of computer time to route the rainfall excess over every particular convolution of the impervious terrain. Secondly, the survey necessary for such a quantity of data would render the model unacceptable to the engineer as a design tool. The only alternative is to undertake an idealisation of the subcatchment shape, in which case the deterministic solution on an appraisal of catchment configuration appears even less justified than the massive data collection mentioned above.

It should be pointed out that the deterministic approach has generally been used in the United States on catchments which are made up of the highly standardised urban block so prevalent in North American cities. On such a catchment, the prodigious data collection and computer time described in the above paragraph are justified on the grounds that the resulting hydrograph can be duplicated several hundred times for the several hundred urban blocks.

The above discussion argues against the use of a deterministic model, when the problem is considered from a purely design viewpoint. However, such an approach will be warranted, in conjunction with some relevant data, as far as any attempt to understand more fully the above-ground phase of the runoff process is concerned. Such an understanding will lead to a better assessment of the merits of any simplified conceptual model which might be considered.

Conceptual approach: The conceptual approach to mathematical modelling uses an alternative, usually simplified, model of the actual prototype process. As such, this approach is preferable to the deterministic approach for the modelling of the complex phenomena which constitute the above-ground phase. Conceptual modelling may be approached from two different philosophies.

The first is the "systems" philosophy. A systems approach to a problem assumes an input and an output to a system, the mechanics of which need bear no resemblance to any of the physical processes involved in the prototype situation. Any alteration to the system mechanics is justified simply in terms of the quality of the output prediction - this, in fact, may be described as a philosophy of "the end justifying the means".

An alternative philosophy, and one which is perhaps more appropriate to the problem on hand, is the one which deals in terms of lumped models and distributed models. A deterministic model is one which attempts to simulate all the particular aspects of a process and may thus be termed a distributed parameter model. On the other hand, a conceptual model may be considered as one which attempts to simulate the process by a simpler concept of the physical system, employing a reduced number of physical parameters to describe the process - in fact, a lumped parameter model.

Storage routing: In hydrology one conceptual approach to mathematical modelling is known as storage routing. It can be described as a lumped parameter approach with storage as the lumped parameter.

The basic equations governing the storage routing concept are as follows

$$\frac{dS}{dt} = i - q \quad \text{- continuity -} \qquad \ldots \quad (1.1)$$

$$S = Kq^n \quad \text{- dynamic -} \qquad \ldots \quad (1.2)$$

where S is the storage in the system

i is the input discharge

q is the output discharge

and t is time.

The above equations may be derived from the St. Venant equations. Equation 1.2 is derived by ignoring the dynamic wave and diffusion wave terms in the St. Venant dynamic equation (in effect, taking the steady uniform flow condition). This is the kinematic wave approximation, which has been shown to be reasonable where lateral inflow predominates (Harley, Perkins and Eagleson, 1970). The overland flow and gutter flow situations are ones which well warrant the kinematic wave assumption.

By differentiating equation 1.2 and substituting for $\frac{dS}{dt}$ in equation 1.1 to eliminate the storage parameter S, we get

$$nKq^{n-1} \frac{dq}{dt} = i - q \qquad \ldots \quad (1.3)$$

There are two possible solutions of equation 1.3, the first for n = 1 and the other for n≠1. The first of these gives a linear relationship between storage and output discharge as may be seen from equation 1.2 This condition is the well-documented case of the linear reservoir, and has been used in the area of urban hydrology by Veissman (1966) on parking lots, and later by the author (1972) on the above-ground phase for developed catchments, and Sarma, Delleur and Rao (1973) for complete catchments. This is in addition to the use of the Unit Hydrograph Theory (of which the linear reservoir is one mathematical description) in the United States by Horner and Flynt (1934). The second case (n≠1) is a less well documented case of a non-linear reservoir, and has been introduced in general terms, but not employed, by Ding (1967). As will be shown at a later point, the latter seems appropriate to the process under consideration. Firstly, however, equation 1.3 will be integrated for the two cases.

The linear reservoir: As has been mentioned above, the linear reservoir is simply one mathematical description of the unit hydrograph

theory. The particular method of application used in this case uses the principle of superposition, which assumes that the nature of the response to any given input pulse is a function only of the pulse and not of the adjacent pulses. As such, a one-minute unit hydrograph may be generated, which is the runoff response to an excess rainfall pulse of one-minute duration and the shape of which is dictated by equation 1.3. The response is assumed to rise linearly to a value q_o at time = 1

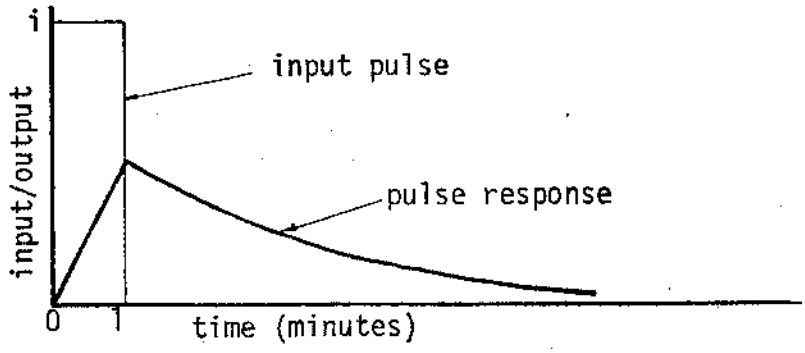

Figure 3: The pulse response model

minute then decay to zero at infinity. The total response is obtained by superimposing the pulse responses. The method adopted in this case is easier to programme than the more rigorous approach adopted in the non-linear reservoir case, and may be shown to produce the same results. The nature of the response decay is obtained from equation 1.3 as follows.

For time t > 1 minute, i=0. Thus together with the assumption that n=1, equation 1.3 reduces to

$$\int_1^t \frac{dt}{K} = \int_{q_o}^{q} \frac{dq}{q} \qquad \ldots \quad (1.4)$$

The solution and simplification of equation 1.4 is

$$q = q_o e^{-(t-1)/K} \qquad \ldots \quad (1.5)$$

By equating the area under the input pulse to the area under the pulse response, the value of q_o may be obtained.

$$q_o = i/(K+0.5) \quad \ldots \quad (1.6)$$

In the particular case under consideration, i is the rainfall intensity (effective) in mm/hour, while q and q_o denote runoff/unit area with units of cumecs/m^2. By allowing for these inconsistent units, the pulse response as shown in Figure 1.3 may be given by

$$q(0) = 0 \quad \ldots \quad (1.7)$$

$$q(1) = i/(K+0.5)/3.6 \times 10^6 \quad \ldots \quad (1.8)$$

$$q(t) = q(1)\ e^{-(t-1)/K} \quad \text{for } t > 1 \quad \ldots \quad (1.9)$$

Parameter K has units of time in minutes, and is the lag time of the pulse response.

According to equation 1.9, the pulse response continues for an infinite time before decaying to zero, and it is thus necessary to have a cutoff point beyond which all ordinates of the response may be effectively ignored. The arbitrary condition for this cutoff point has been chosen as being that point which includes 99% of the total area under the recession limb of the response. The area beneath the decay between time = T and infinity may be shown to be equal to $K\ q_o e^{-T/K}$, where T is measured from the end of the pulse. It follows that the total area under the decay is equal to $K\ q_o$. A value for the cutoff time T may be obtained by equating the two areas in the following manner

$$\frac{K\ q_o\ e^{-T/K}}{K\ q_o} = 0.01 \quad \ldots \quad (1.10)$$

Equation 1.10 reduces to

$$T = 4.60\ K \quad \ldots \quad (1.11)$$

Knowing the value of K, it is now possible to calculate a value of T beyond which the response ordinates may be considered to be negligible.

In generally accepted unit-hydrograph methodology the process adopted may be considered as multiplying the ordinates of the one-minute unit hydrograph by the size of the input. Since the principle of convolution applies, then the total response hydrograph may be obtained by adding the responses of one-minute intervals of rainfall input as demonstrated by Figure 4. The inlet hydrograph may then

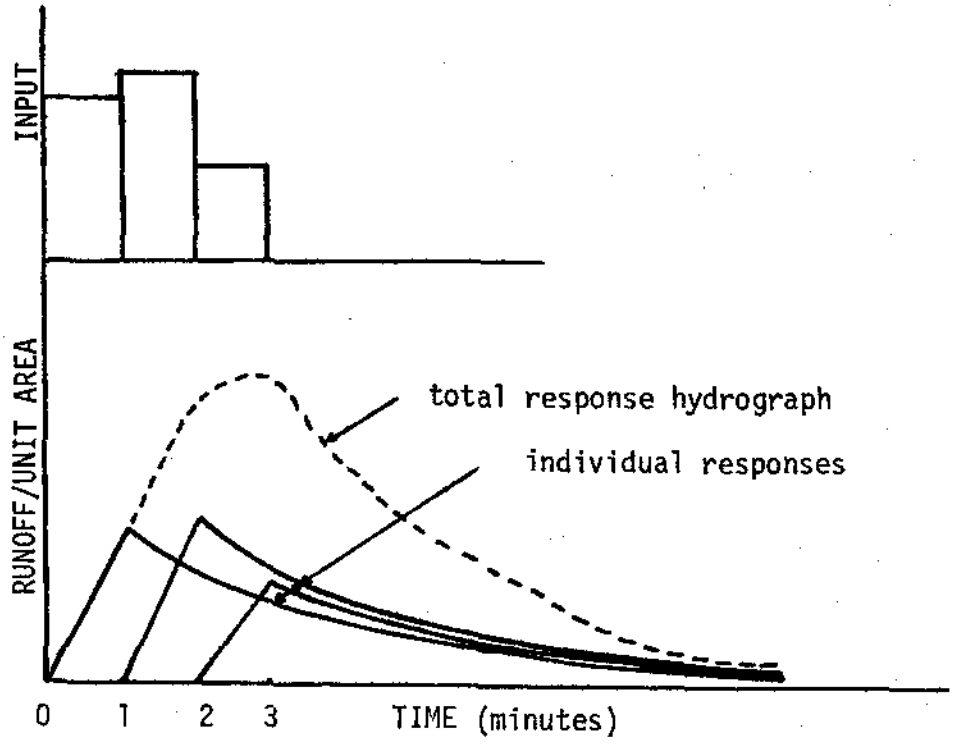

Figure 4: The total response hydrograph

be simply obtained by multiplying the ordinates of the total response hydrograph by the area of given surface type contributing to the given inlet.

The non-linear reservoir: In the case of the non-linear reservoir, the principle of convolution no longer exists and, as such the pulse response mechanism will no longer work as a solution to equation 1.3. The nature of the system response to an input pulse in this case is as much a function of the adjacent input as the input itself. It should be said that such a pulse response model could produce a non-linear solution, but that it would not be the non-linear model which equations 1.1 and 1.2 suggest; and it is unlikely that such a model could simulate the surface routing phenomena as successfully as the model postulated in this section, as will be demonstrated later. There are two possible solutions to equation 1.3, one for $i \neq 0$ and the other for $i=0$.

For the case where it is still raining ($i \neq 0$), the solution of equation 1.3 is achieved by determination of output q over successive time intervals T (see Figure 5) during which the input rainfall intensity may be assumed to be constant (this latter is in fact convenient, since the rainfall hyetograph is in the form of constant rainfall intensities

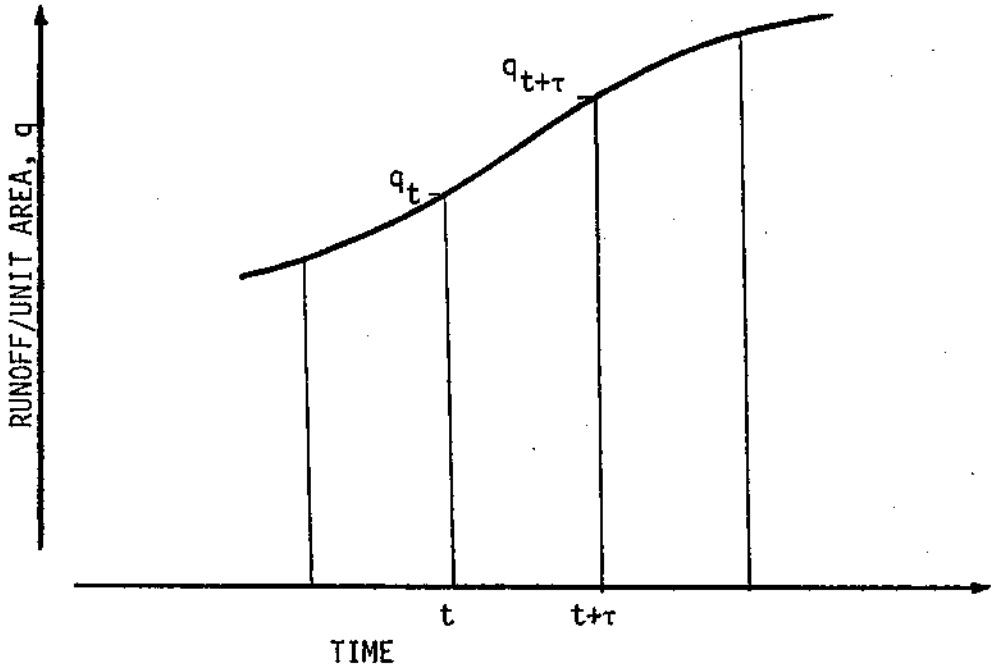

Figure 5: Successive determination of output q during rainfall

of one minute duration, and as such the solution may be seen as being an exact solution of the given input). Equation 1.3 may be converted to the following convenient form

$$\int_{q_t}^{q_{t+\tau}} \frac{q^{n-1}\,dq}{i-q} = \frac{1}{nK} \int_{t}^{t+\tau} dt = \frac{\tau}{nK} \qquad \ldots \quad (1.12)$$

By making the substitution $u = (q/i)^n$ to the left hand side of equation 1.12, it may be simplified to

$$i^{n-1} \int_{u_t}^{u_{t+\tau}} \frac{du}{1-u^{1/n}} = \frac{\tau}{nK} \qquad \ldots \quad (1.13)$$

The left hand side of equation 1.13 may be divided up to give

$$\int_0^{u_{t+\tau}} \frac{}{1-U^{1/n}} - \int_0^{u_t} \frac{du}{1-U^{1/n}} = \frac{\tau}{nKi^{n-1}} \qquad \ldots \qquad (1.14)$$

The integral $\int \frac{du}{1-U^{1/n}}$ is Bakhmeteff's Varied Flow Function (VFF).

The varied flow function is well known to hydraulicians and appears in many solutions of backwater curve problems. It has no analytical solution, although Bakhmeteff (1932) has given a number of approximate methods for its solution. Chow (1959) has tabulated the VFF for various values of n, none of which are of the magnitude to be expected for the purposes of this model. However, Bakhmeteff gives two infinite series, one for values of u on each side of unity, which converge swiftly for all values except those very close to unity.

The two series for the solution of Bakhmeteff's varied flow function are given as follows. The value of m is equal to 1/n, where n is the value of nonlinearity in the text. For $U < 1$,

$$\int \frac{du}{1 - U^m} = U + \frac{1}{m+1} U^{m+1} + \frac{1}{2m+1} U^{2m+1} + \ldots\ldots\ldots$$

$$\ldots\ldots + \frac{1}{(p-1)\,m+1} U^{(p-1)m+1} + Rp \qquad \ldots \quad (1.15)$$

$$\text{where } Rp < \frac{U^{pm+1}}{pm+1} \cdot \frac{1}{1-U^m} \qquad \ldots \quad (1.16)$$

For $U > 1$,

$$\int \frac{du}{1 - U^m} = \frac{1}{(m-1)U^{m-1}} + \frac{1}{(2m-1)U^{2m-1}} + \ldots\ldots\ldots$$

$$\ldots\ldots + \frac{1}{((p-1)m-1)U^{(p-1)m-1}} + Rp \qquad \ldots \quad (1.17)$$

$$\text{where } Rp < \frac{1}{(pm-1)U^{pm-1}} \quad \frac{U^m}{U^m - 1} \qquad \ldots (1.18)$$

Equations 1.16 and 1.18 allow us to determine the number p of the members of the series. The closer to unity the value of u becomes, the greater the number of terms in the series necessary for convergence.

Knowing the values of q and i at time t, it is now possible to calculate the value of u and the VFF (from one of the above mentioned series) at time t, and then, from equation 1.14, to calculate the VFF at time t+τ. Unfortunately, there is no series to calculate the value of u from the VFF. It is thus necessary either to use an iterative technique to determine u from the VFF by successive approximations, or to tabulate values of the VFF against u for a given value of n and to determine values by a simple scan. The former is attractive but could be very time-consuming on even a fast computer if the solution does not converge swiftly. The latter limits the model user to only those values of n which he chooses to tabulate, but is considered to be preferable under the circumstances. (The quasi-physical justification for the value of n which appears later in the chapter also supports this last choice of methods.) Having determined u for time t+τ from the table, then $q_{t+\tau}$ may be calculated. The value of $q_{t+\tau}$ then becomes q_t for the next time interval and i taken as the rainfall intensity during the next interval, and the procedure repeated. This method is repeated through the duration of the rainstorm.

When there is no rainfall, then equation 1.3 becomes a much simplified formula, for which, as in the case of the linear reservoir, there is a direct solution. Equation 1.3 now becomes

$$-\int_{q_t}^{q_{t+\tau}} q^{n-2}dq = \frac{1}{nK}\int_{t}^{t+\tau} dt \qquad \ldots (1.19)$$

thus

$$q_{t+\tau}^{n-1} - q_t^{n-1} = \frac{n-1}{n}\cdot\frac{\tau}{K} \qquad \ldots (1.20)$$

Simplifying equation 1.16 and using τ = 1 minute as a suitable time increment, we get

$$q_{t+1} = q_t\left[1 - \frac{(1-1/n)}{Kq_t^{n-1}}\right]^{1/(1-n)} \text{ for } i=0 \qquad \ldots (1.21)$$

Equation 1.14 and 1.21 represent the application of the non-linear reservoir model to the surface routing part of the above-ground model.

The values of q obtained are divided by the conversion factor 3.6 x 10^6, as for equation 1.8, to give them in the required units of cumecs/m^2. As in the case of the linear reservoir, the inlet hydrograph may now be obtained by multiplying the ordinates of the total response hydrograph (generated from equation 1.14 and 1.21) by the area of specified surface type contributing to any given inlet.

The degree of non-linearity of the conceptual model: It is advantageous at this point to assess the likely degree of linearity or non-linearity of the conceptual model for the surface routing model. It may be possible to postulate an optimum assessment of the model parameter n before studying the complete simulation procedure.

Accepting that overland flow is the predominant facet of the above-ground phase, it has been found that the overland flow phenomenon is itself non-linear. Musik (1974) studied the behaviour of a tilted impervious surface under rainfall in the laboratory and demonstrated that a unit hydrograph approach to the solution, which inherently assumes linearity, was unsuccessful as a prediction technique. On the other hand, he demonstrated that the kinematic wave approximation to the full St. Venant equations led to an effective prediction technique, albeit in the laboratory. The kinematic wave approximation leads to a steady state version of the St. Venant dynamic equation, which itself leads to a non-linear discharge-storage relationship. The exact nature of this relationship may be obtained by application of Chezy's equation to a channel in which the width is very great in comparison to the depth. In this circumstance, the value of the non-linearity parameter n for overland flow (fully turbulent) is 0.67. If the gutter flow may be assumed to be flow in a wide channel, then the same value of n may apply. The same approach using an assumption of laminar flow leads to a value of the parameter n equal to 0.33. However, it would seem likely that the flow regime will be turbulent, particularly under rainfall.

Having recognised the non-linearity of the predominant features, this does not in itself guarantee the same non-linearity of the complete process, although it does promise some degree of non-linearity. However, there is evidence to suggest that the whole process is non-linear. It has been found that the response of the small catchments studied in this work, inclusive of sewer flow, is itself non-linear, as demonstrated in Figure 6. The recession limbs would be straight lines when plotted semi-logarithmically if the discharge-storage relation were linear. The below-ground phase is close to being a linear system, and, by the argument that the non-linearity of a part will produce a non-linearity of the whole, the above-ground phase must be non-linear.

The author's experience of studying other catchments tends to suggest that, by using a linear approach to the above-ground phase, it is not possible to successfully simulate both the peak of the hydrograph and its recession limb. This may be corrected by using a non-linear reservoir, where the nature of the response depends on the size of the input. It is the purpose of this study to test the viability of the non-linear reservoir model, with non-linearity n equal to 0.67, and to compare its performance with the simpler linear reservoir model.

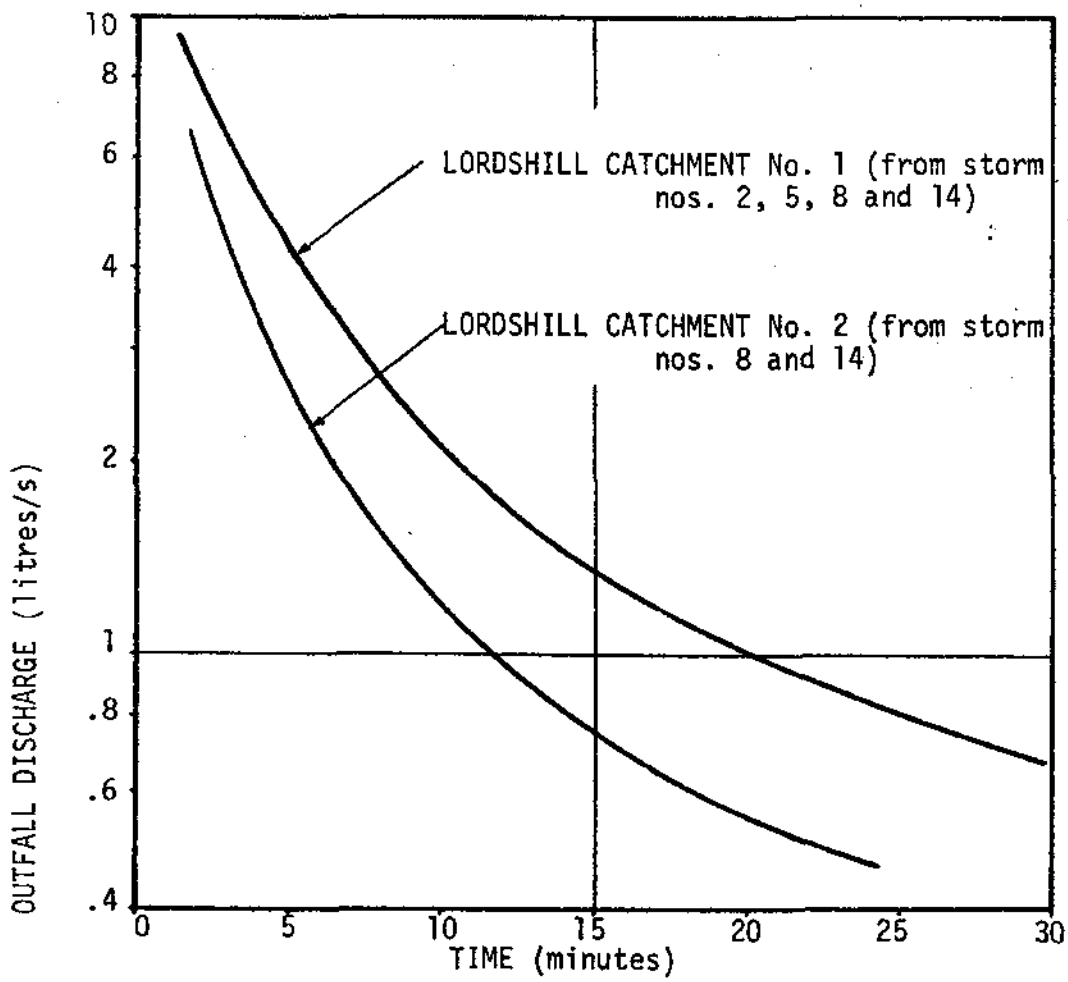

Figure 6: Recession limbs, plotted logarithmically

Time of entry submodel: A further simplistic model was tried as an alternative to the nonlinear and linear reservoir models for surface routing. General practice in design in this country recommends a 2-minute time of entry for routing the rainfall excess prior to entry to the sewer system. Effectively, this consists of multiplying the rainfall excess by the contributing area and lagging the result by 2 minutes to obtain the inlet hydrograph.

II: THE BELOW-GROUND MODEL

Unlike the above-ground phase with its complex combination of unclearly defined physical phenomena, the modelling of the below-ground phase lends itself well to a deterministic approach. Pipe flow is a clearly defined physical phenomenon and is the predominant feature of the below-ground phase.

The modelling of the below-ground phase may be seen as a process of combining and routing the inlet hydrographs through the sewer system to the outfall. The first requirement for the model is a description of the sewer network, and this is achieved by the following numbering system, as demonstrated in Figure 7.

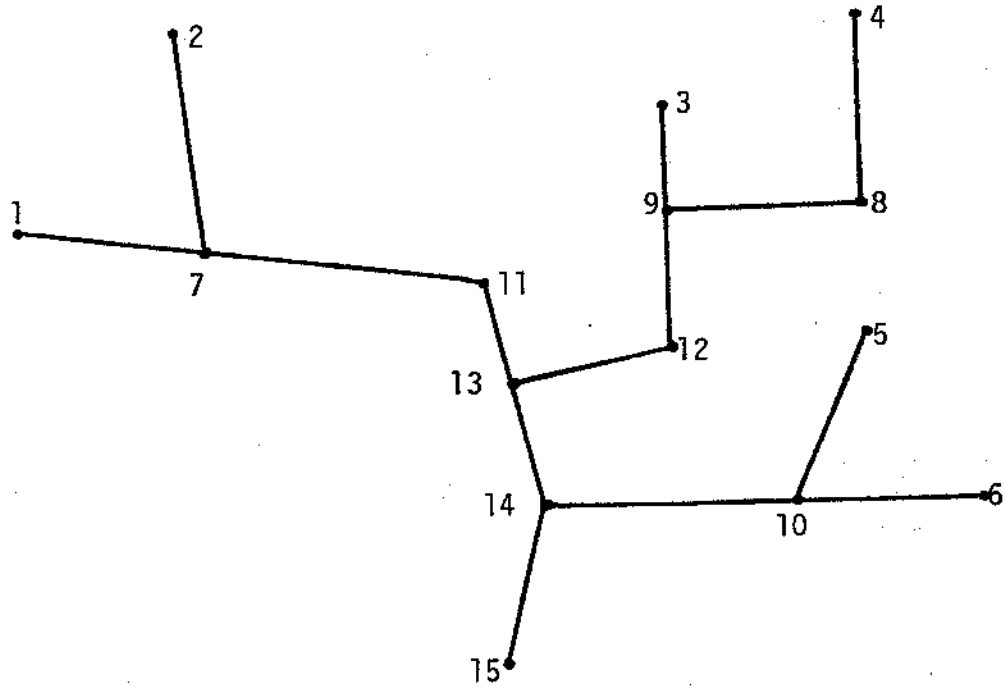

Figure 7: Example of sewer network numbering system

The network junctions are numbered, the only criterion being that, above a given junction, there shall be no junction having a number greater than its own. In effect, this may be achieved by numbering

it is valuable to consider briefly the underlying assumptions inherent in the derivation.

ASSUMPTIONS RELATING TO THE ST. VENANT EQUATIONS: The main assumption in the derivation is that vertical accelerations are negligible in comparison to the horizontal accelerations. This assumption requires that the equations only be used for "long" waves (the steeper the wave the less justified the assumption), and, as such, they cannot be expected to cope with storm surges and standing waves. Two related assumptions are that the vertical velocity distribution is the same as for steady uniform flow at the same depth, and the friction resistance is the same as for steady uniform flow at the same depth. These two are only justified for long waves where gradually-varied flow conditions apply. The last assumption is that the conduit slope is small, such that $\sin(i) = \tan(i) = i$ and $\cos(i) = 0$, where i is the angle of slope. The latter also implies that the hydrostatic pressure distribution lies along a vertical.

The individual effects of the preceding assumptions are difficult to investigate in detail, let alone to quantify in any way. However, research at Colorado State University (Yevjevich and Barnes, 1970) has indicated that the full St. Venant equations are applicable to the solution of long waves in circular conduits.

SOLUTION OF THE ST. VENANT EQUATIONS: Since Stoker first used the St. Venant equations in 1953 for flood routing, many schemes have been proposed for their solution, none of which has particularly stood out from the rest. They may be broadly categorised into three types, implicit, explicit and characteristics schemes. The explicit schemes, as typified by the Lax-Wendroff method employed by Liggett and Woolhiser (1967), form the most common category. The implicit type, the best example of which is that proposed by Amein (1968), has a tendency to be somewhat time-consuming but does not have the same stability problems experienced with the explicit type. The characteristics schemes, as typified by the method given below, tend to be largely stable. In general, it is fair to say that there is little difference between the various schemes in terms of accuracy, and an assessmentof the applicability of the different methods is given by Price (1974) for routing in natural channels.

The choice of the fixed-grid characteristics scheme is not intended as any judgement on the relative merits of the methods mentioned above; further, it is not the intention to investigate the phenomenon of gradually-varied flow in sewers but to employ a method in which it is possible to be relatively confident in terms of accuracy. The method of characteristics provides such a vehicle.

THE METHOD OF CHARACTERISTICS: The method of characteristics is used in a wide variety of fields for the solution of propagation problems. Mathematically it may be considered as a means of solving simultaneous partial differential equations, but it is useful to look at the problem from a more fundamental viewpoint.

first the remote inlets and then inwards from the tip of the 'tree' to its 'trunk'.

The individual inlet hydrographs are generated (according to the previous chapter) for the remote inlets. Each of these hydrographs is then routed through the interconnecting pipe to the junction below, the junction hydrograph of which comprises the summation of any routed hydrographs and its own inlet hydrograph. This junction hydrograph is then routed through the next interconnecting pipe, and the process repeated through the network to the outfall.

We now consider the routing of a hydrograph through a given stretch of pipe. Backwater effects at junctions and surcharging are not taken into account by the model, although it is recognised that these phenomena may be important in some situations. In the event, the pipe systems used here are of such a slope that these effects are unlikely to be important. The hydrograph routing is achieved by one of two models, as described below, the first of which is a complex and time-consuming exercise while the second may be seen as a simplification. It will also be explained that, under certain high energy situations, it is necessary to employ the second model because the solution of the first model becomes unstable.

The Characteristics Pipe-routing Method

The general equations relating to long waves in open channels with no lateral inflow are the St. Venant or "shallow water" equations and may be defined as

$$\frac{g\partial h}{\partial x} + \frac{\partial v}{\partial t} + v\frac{\partial v}{\partial x} = g(s_o - s_f) \quad \text{- equation of motion -} \quad \ldots (2.1)$$

$$A\frac{\partial v}{\partial x} + v\frac{\partial A}{\partial x} + \frac{\partial A}{\partial t} = 0 \quad \text{- equation of continuity -} \quad \ldots (2.2)$$

where h is the water depth

x is the distance in the downstream direction

v is the velocity

t is the time

s_o is the channel slope

s_f is the friction slope

and A is the cross-sectional area of flow.

Equations 2.1 and 2.2 have been derived many times and are presented in a multitude of different forms. There are also several methods of solution, all of which are based on some form of finite-difference technique. While avoiding the tedium of deriving the above equations,

By definition, a "characteristic" is a path along which an entity may be propagated. In the particular situation of long waves in open channels, the entity may be seen as a discrete disturbance in an x-t plane (Figure 8), where x is the distance measured in the downstream direction and t is time.

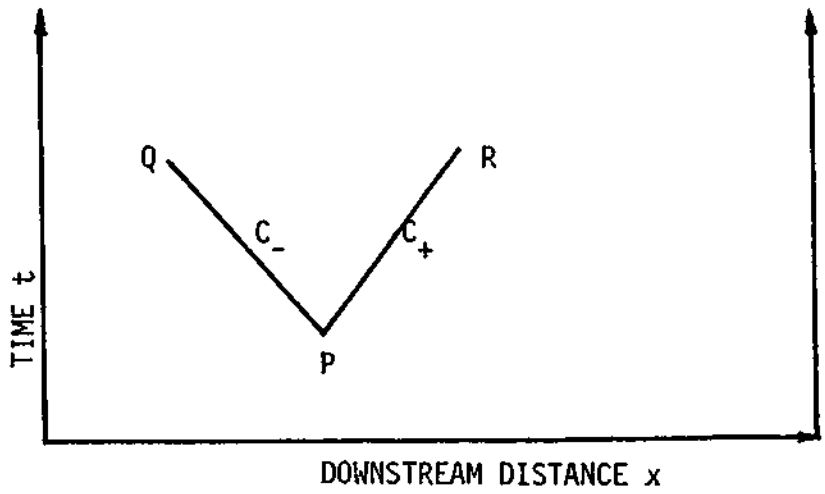

Figure 8: The x-t plane

From a point P, a disturbance may be propagated in two directions, downstream towards point R (C_+ characteristic) and upstream towards point Q (C_- characteristic), although it will be seen later that for conditions of supercritical flow the C_- characteristic will also be propagated in the downstream direction. The area in the x-t plane bounded by the line QPR is the zone of influence of point P.

By considering a water depth associated with every point in the x-t plane, it is possible to imagine an "integral surface" with the characteristics embedded in it, in fact, describing it. Since there is a distinct difference in the zones of influence each side of any characteristic, it follows that the slope of the integral surface across this characteristic may be discontinuous, and it follows again that the first derivatives of the equations describing the variation of depth with time and distance may also be discontinuous and thus indeterminate. The St. Venant equations are such descriptions of the first derivatives, and as such the conditions under which they are indeterminate will define the direction and nature of the characteristic. It is thus necessary to define those conditions under which the St. Venant equations are indeterminate. A more explicit discussion of the fundamentals of the method of characteristics is provided by Abbott (1966), who applies the method to a variety of engineering problems.

Equations 2.1 and 2.2 are first converted into a form using discharge, Q, and cross-sectional area, A, instead of v and h. The concept of an integral surface still applies, if no longer so easy to visualise.

The only problem associated with this conversion is involved with the $\frac{\partial h}{\partial x}$ term in equation 2.1. If A = f(h), where f is some function, then it follows that $\frac{\partial A}{\partial x} = f'(h)\frac{\partial h}{\partial x}$. It may be shown that, if A = f(h), then for any given cross-section, f'(h) is equal to the surface width, B. When converted, equations 2.1 and 2.2 become

$$(\frac{A^3 g}{B} - Q^2)\frac{\partial A}{\partial x} + QA\frac{\partial Q}{\partial x} - QA\frac{\partial A}{\partial t} + A^2\frac{\partial Q}{\partial t} = A^3 g(s_o - s_f) \quad \ldots \quad (2.3)$$

$$\frac{\partial Q}{\partial x} + \frac{\partial A}{\partial t} = 0 \quad \ldots \quad (2.4)$$

To complete the system of equations defining the integral surface, we have the equations of variation:

$$\frac{\partial Q}{\partial t}.dt + \frac{\partial Q}{\partial x}.dx = dQ \quad \ldots \quad (2.5)$$

$$\frac{\partial A}{\partial t}.dt + \frac{\partial A}{\partial x}.dx = dA \quad \ldots \quad (2.6)$$

Equations 2.3, 2.4, 2.5 and 2.6 may be written in matrix notation;

$$\begin{bmatrix} (\frac{A^3 g}{B} - Q^2) & -QA & QA & A^2 \\ 0 & 1 & 1 & 0 \\ 0 & 0 & dx & dt \\ dx & dt & 0 & 0 \end{bmatrix} x \begin{bmatrix} \frac{\partial A}{\partial x} \\ \frac{\partial A}{\partial t} \\ \frac{\partial Q}{\partial x} \\ \frac{\partial Q}{\partial t} \end{bmatrix} = \begin{bmatrix} A^3 g(s_o - s_f) \\ 0 \\ dQ \\ dA \end{bmatrix} \quad \ldots \quad (2.7)$$

The first of the two conditions governing the discontinuity of these two equations is that the determinant of the 4x4 matrix on the left hand side of the equation is equal to zero. This condition reduces to the following quadratic equation

$$(\frac{dx}{dt})^2 - 2\frac{Q}{A}\frac{dx}{dt} - (\frac{Ag}{B} - \frac{Q^2}{A^2}) = 0 \quad \ldots \quad (2.8)$$

The solution of this quadratic equation is

$$\frac{dx}{dt} = \frac{Q}{A} \pm \sqrt{\frac{Ag}{B}} \qquad \ldots \quad (2.9)$$

Equation 2.9 defines the slope of the characteristic in the x-t plane, the positive root referring to the C^+ characteristic and the negative root to the C^- characteristic. It is also worthy of note that the term $\sqrt{\frac{Ag}{B}}$ is the wave celerity or the velocity of propagation of a disturbance in a stationary medium with a free surface. Thus the value of $\frac{dx}{dt}$ is given by the wave celerity corrected by the water velocity, $\frac{Q}{A}$.

The second condition of indeterminancy is that the determinant given by the 4 x 4 matrix and the right hand side vector is equal to zero, or

$$\begin{vmatrix} (\frac{A^3 g}{B} - Q^2) & -QA & QA & A^2 & \{A^3 g(s_o - s_f)\} \\ 0 & 1 & 1 & 0 & 0 \\ 0 & 0 & dx & df & dQ \\ dx & dt & 0 & 0 & dA \end{vmatrix} = 0 \qquad \ldots \quad (2.10)$$

The matrix equation 2.10 reduces to

$$\frac{dQ}{dt} = Ag(s_o - s_f) - (\frac{Ag}{B} - \frac{Q^2}{A^2}) \frac{dA}{dx} \qquad \ldots \quad (2.11)$$

Equation 2.11 is known as the Riemann Invariant, and may be applied along either characteristic.

The solution is completed by a definition of the friction slope, s_f, and Manning's Formula is employed, assuming no variation in Manning's n with depth. This relation is given by

$$s_f = \frac{n^2 V|V|}{R^{1.33}} \qquad \ldots \quad (2.12)$$

where R is the hydraulic radius of the cross-section.

Equations 2.9, 2.11 and 2.12 provide the basis of the solution by the method of characteristics, and may be solved through the x-t plane

by a finite difference technique.

PROGRAMMING OF THE METHOD OF CHARACTERISTICS: The method of characteristics solution is programmed on a fixed finite difference grid, as indicated in Figure 9. RP is the C_+ characteristic and SP the C_- characteristic. The dotted line $S^{\dagger}P$ will be the C_-

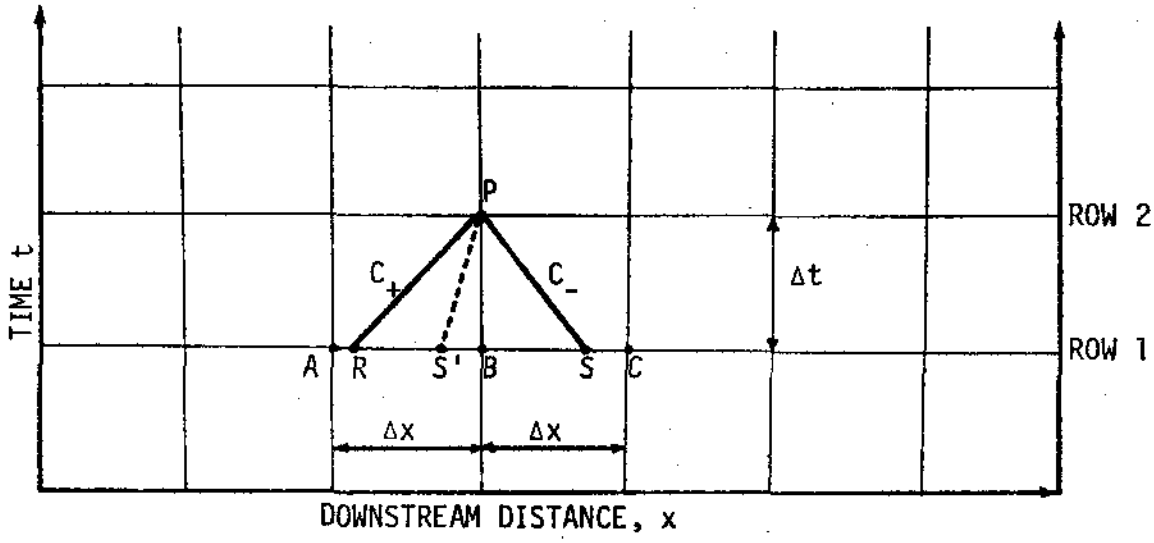

Figure 9: The fixed finite difference grid

characteristic under supercritical conditions, or when $\frac{Q}{A}$ is greater than $\sqrt{\frac{Ag}{B}}$ in equation 3.9.

If the values of Q, A, V, etc are known at points A, B and C in the fixed grid, then those values at R and S may be found by quadratic interpolation. Then, using a finite difference form of equations 2.9 and 2.11, it is possible to calculate values of Q, A, V, etc. at point P. This procedure is carried out for all points in row 2 of the grid (the boundary conditions are required for the extreme values of x). Given the correct boundary conditions, it is possible to extend the method through successive time increments in the x-t plane until a complete description of the behaviour is achieved.

BOUNDARY CONDITIONS: There are three boundary conditions which correspond to the three boundaries of the x-t plane. The first boundary condition refers to the flow regime at the commencement of the solution, or the values of Q, A, V, etc. at time equal to zero for all values of x.

The second boundary condition refers to the upstream vertical boundary of the x-t plane, and is the input hydrograph to the conduit reach.

The requirement is a discrete relation between the input discharge, Q, and time, which is in fact the input to the system, the output being a discrete relation between the downstream discharge and time.

The final boundary condition refers to the downstream vertical boundary of the x-t plane, and is a relation between the discharge and the physical restraints at the downstream boundary. This may be, say, a weir condition pertaining to a free overfall, or, as has been chosen here, a condition relating to steady uniform flow. It is doubtful that a change in downstream condition would make an appreciable difference to the downstream hydrograph. Where supercritical flow conditions occur, this boundary condition reverts to the upstream boundary. This is explicable by the fact that there is no longer an upstream facing characteristic by which to define the conditions at the upstream boundary, and by the fact that, under these conditions, the precise nature of the downstream boundary is irrelevant to the flow immediately prior to it.

CHOICE OF THE GRID SIZE: The size of the time grid spacing (Δt in Figure 9) is given by the Courant Condition (Courant *et al.*, 1952). It is desirable that R and S should lie between A and C in Figure 9. This condition is satisfied by the slope of the C^+ characteristic being greater than the ratio $\frac{\Delta t}{\Delta x}$. Thus the Courant Condition states that

$$\Delta t < \Delta x/(\frac{Q}{A} + \sqrt{\frac{Ag}{B}}) \qquad \ldots \quad (2.13)$$

where values of Q, A and B may be assumed to be those values at point B. Since Δt refers to all the points in any row, it is desirable to select the least value of Δt found from the Courant Condition applied to all the points in any row. Thus Δt may vary with time but not with distance.

There is little information concerning the optimum value of Δx in the relevant literature. It is clear that as its value decreases we get closer to an exact solution while the computation time necessary increases. A brief sensitivity analysis was undertaken to ascertain a suitable value for Δx, the results of which are indicated in Figure 10.

A hypothetical storm was routed through a hypothetical pipe with a slope of 0.5%, diameter 9 inches and length 100 ft such that the flow regime was subcritical. It was surmised that a suitable value of Δx was 6 metres. Values much greater than this led to inaccuracy in the routed hydrograph, while values much less produced a very small increase in accuracy with a considerable increase in computation time.

PRACTICAL PROGRAMMING LIMITATIONS: There are two minor programming limitations found with a method which is for the most part stable. The first limitation is found for small depths of flow. Small changes in depth in this region produce relatively large changes in cross-sectional area, which produces an instability in the calculation of velocity. This instability is corrected by the introduction of a small

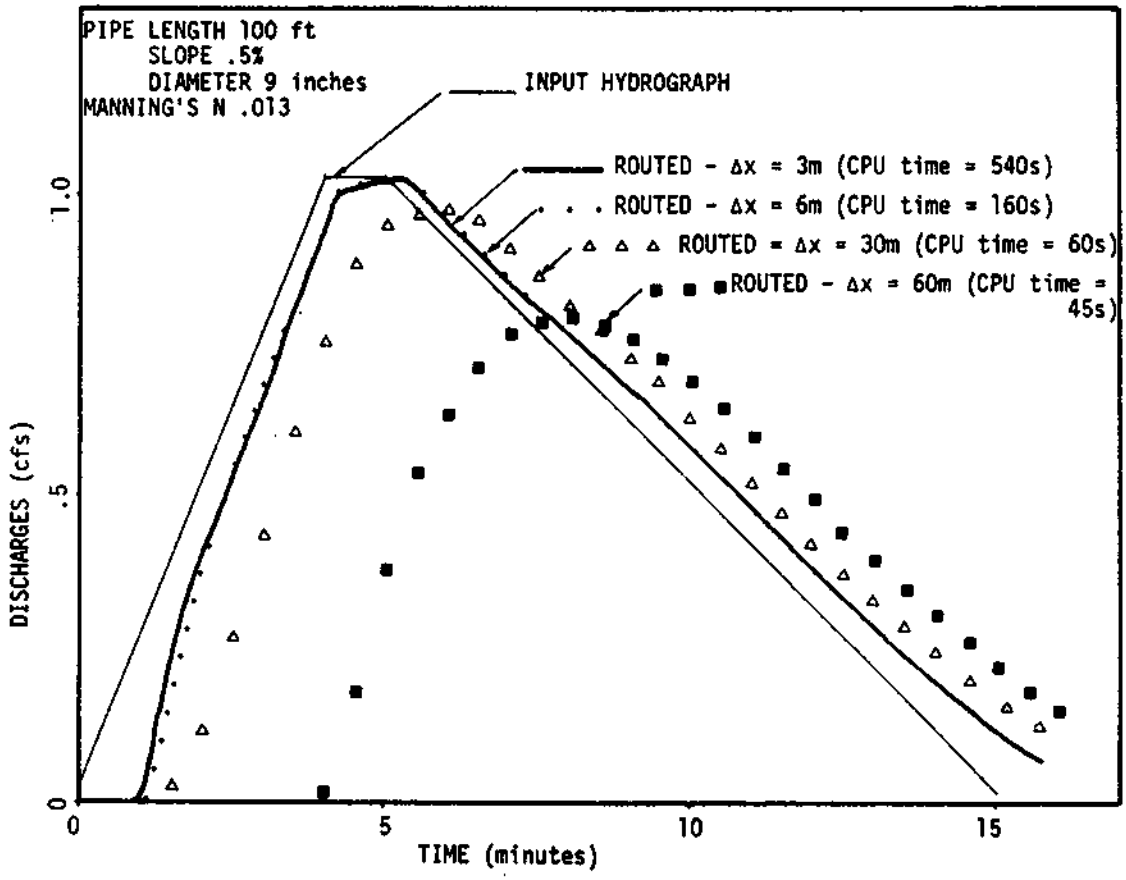

Figure 10: Sensitivity analysis for grid spacing Δx

base flow, which has a negligible effect on the remainder of the hydrograph. This base flow is introduced whenever the input discharge is below a threshold value.

While the above may be seen as a mathematical instability, the second limitation is caused by more fundamental considerations. It has been found that the St. Venant equations break down for Froude numbers in excess of about 2.0. It is difficult to say for certain why the solution breaks down under these circumstances, but it is perhaps due to the St. Venant assumptions discussed earlier no longer being valid. The limitation manifests itself by an instability which occurs at different points in the x direction, causing faulty results without necessarily a complete breakdown of the procedure. This particular area of the model has therefore to be approached with some caution since it is possible to get faulty results without knowing it. In this circumstance, it is necessary to resort to a simplified method of pipe-routing, as described in the next section. The necessity for using the simplified approach for any given hydrograph in any given pipe is ascertained by calculating the Froude number corresponding to steady uniform flow with the peak of the hydrograph as the discharge value.

The kinematic pipe routing method: As has been explained,the St. Venant equations break down for high Froude numbers of the order of 2 and greater. Such high energy situations tend only to occur in steep sewers likely to be found at the tip of a sewer system.

The kinematic approximation to the St. Venant equations ignores the three terms on the left hand side of the equation of motion (Equation 2.1). The first of these terms, $g\frac{\partial h}{\partial x}$, is the diffusion term, the second, $\frac{\partial v}{\partial t}$, is the acceleration term, and the third, $v\frac{\partial v}{\partial x}$, is the dynamic term. They combine to provide the effect of retention due to the storage of the channel. It seems likely that, under the high energy conditions which occur when this method is being employed, the effect of storage will be reduced due to the high velocity. This factor would tend to support the use of the kinematic method at high Froude numbers, irrespective of the breakdown of the characteristics method.

When the left hand side of Equation 2.1 is ignored, then the right hand side of the equation simply gives an expression relating discharge to slope and hydraulic radius, which is in fact the accepted equation for steady uniform flow in an open channel. The ordinates of the input hydrograph are thus offset by a time corresponding to the velocity of flow pertaining to that discharge, as defined by Manning's formula. The process is demonstrated in Figure 11.

A further method was considered, known as the Time Offset Method (Tholin and Keifer, 1960), which has in the past been popular in North America. In this method, the whole hydrograph is offset by a representative time, calculated from representative discharge as applied to Manning's formula. The justification for this method was that the hydrograph shape was unlikely to alter greatly down one length of pipe. The weakness of this argument is that the small change in hydrograph shape is likely to become appreciable when applied to a great number of pipes. The kinematic method was preferred, as it is no more difficult to program, and, as has been suggested above, it may be an excellent approximation under high energy conditions.

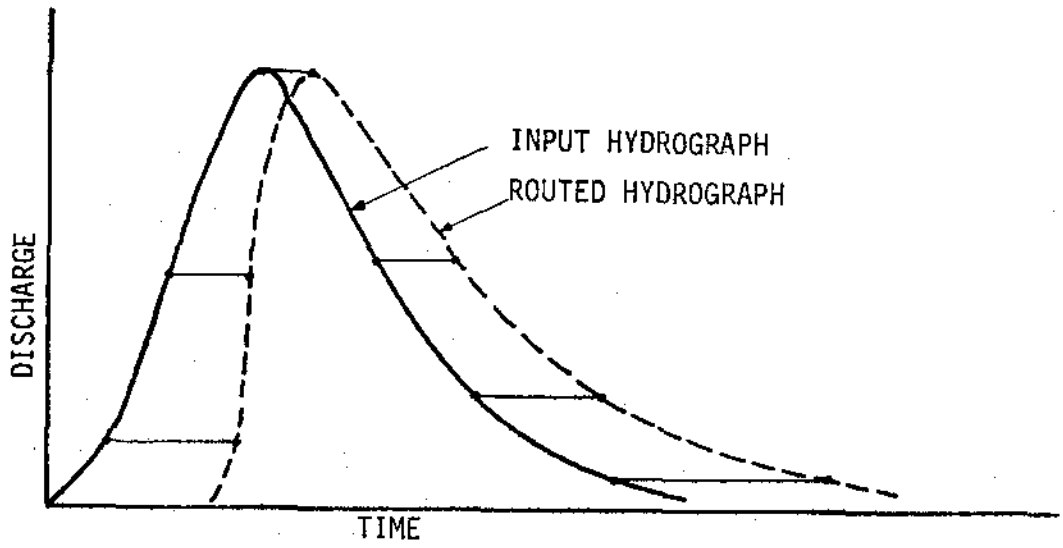

Figure 11: The Kinematic Pipe-routing Method.

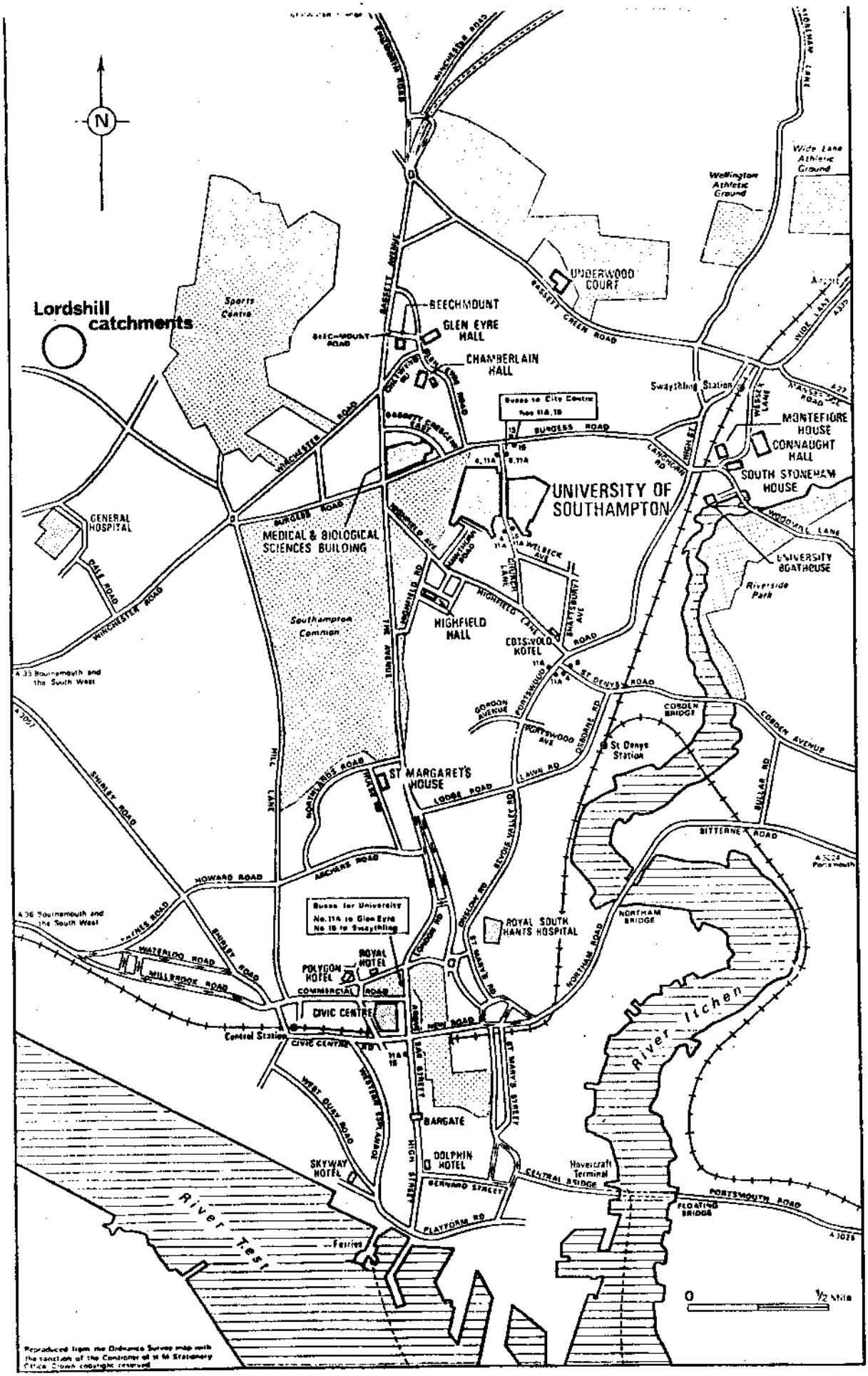

Figure 12: Location map for Lordshill catchments

III : DATA COLLECTION PROGRAMME

As has been discussed earlier, it was recognized that there was a requirement for rainfall-runoff data at or close to the boundary between the above-ground and below-ground phases of the urban runoff process. Two small adjacent catchments were found which fulfilled the criteria for such a study, and a data collection programme commenced at the beginning of 1974. The first few months of the programme were spent in establishing the necessary instrumentation, and then the two catchments were monitored continuously for rainfall and runoff from 11 June 1974 to the present time apart from a three-month break between late December 1974 and mid-March 1975. (Events of sufficient intensity are very unlikely to occur during this period). Storm events up to the end of August 1975 are included in this particular study, but the programme is continuing and may be expanded in the near future.

The two catchments are located in Lordshill, a recent residential development on the northern outskirts of the City of Southampton. The situation of the two catchments is shown on the location map in Figure 12. The catchments form part of an estate of which they comprise about a quarter of the total area. At the beginning of 1974, the two catchments were the only portions of the estate which had been completed. Stormwater drains from the remainder of the estate through a different sewer system from the two systems in the catchments in question.

Figure 13 is a map of the two catchments and shows the outline of the roads, footpaths and driveways, the outline of the roofed areas, and the lines of the storm sewer systems draining each of the two catchments. Both sewer systems outfall into a tributary of Tanner's Brook, and the runoff is gauged at these two points. The location of the instrumentation cabin may be seen halfway between the two outfalls. Figure 14 is a view of the instrumentation cabin as seen from the north.

The more northern of the two catchments has been named Lordshill Catchment number 1, and drains to outfall number 1. It comprises Curlew Close and a portion of Sandpiper Road. It has a gross area of about 8000 m^2 and an impervious area of 3337 m^2, of which 2255 m^2 is pavement (roads, footpaths, driveways) and 1082 m^2 is roofed area. It has a fairly steep average ground slope of 3.0%. Figure 14 is a view of Curlew Close looking in the direction of the outfall from a position close to the manhole at which the main "drag" of the sewer system turns through a right angle towards Sandpiper Road.

The more southern of the two catchments has been named Lordshill Catchment number 2, and drains to outfall number 2. It drains all of Fulmar Close. It has a gross area of 6000 m^2 and an impervious area of 2523 m^2, of which 1256 m^2 is pavement and 1266 m^2 is roof.

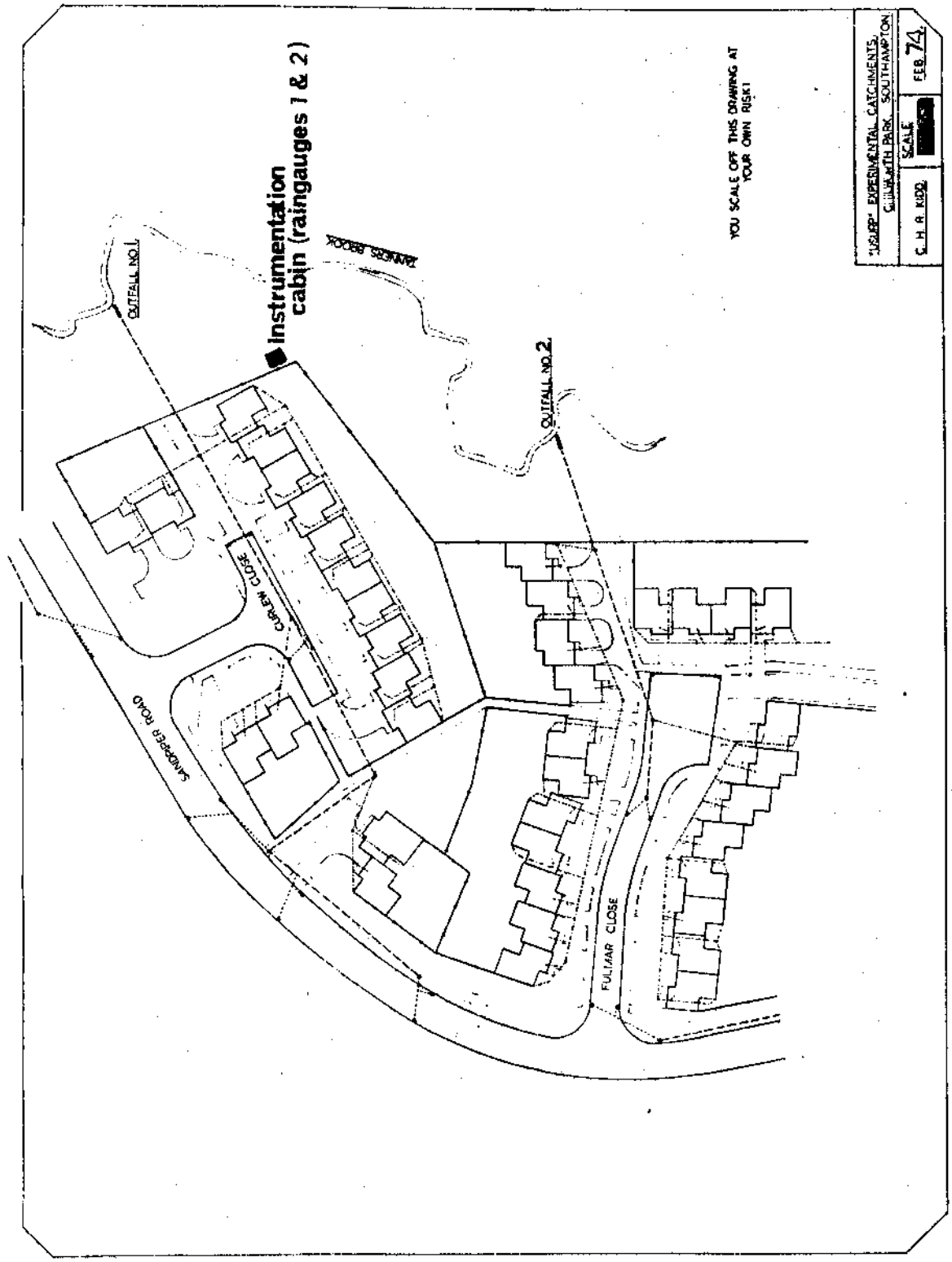

Figure 13: Lordshill catchments Nos. 1 and 2.

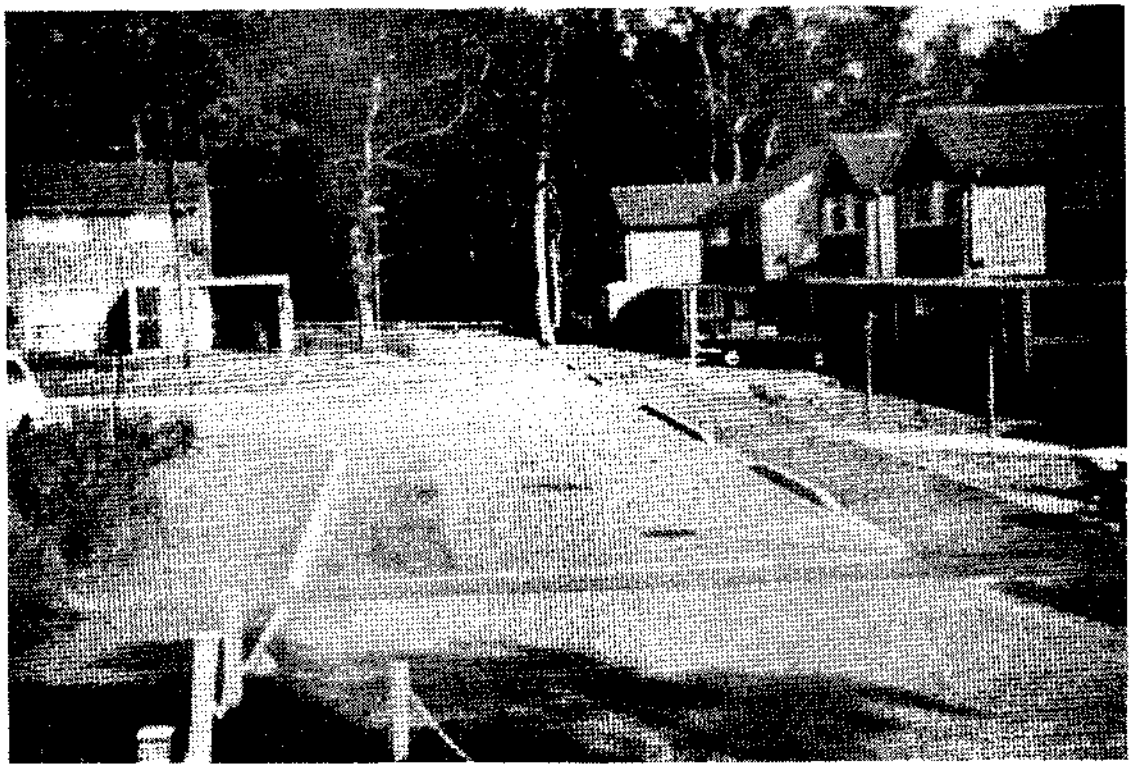

Figure 14: View of Lordshill catchment No. 1

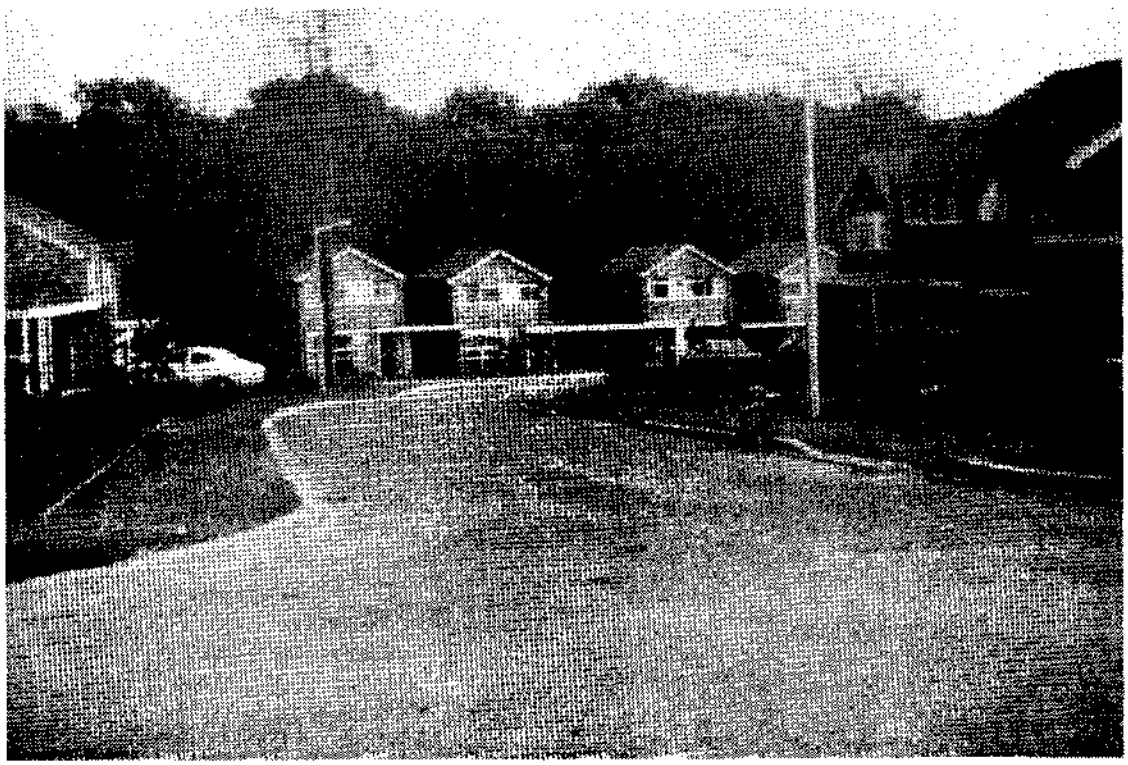

Figure 15: View of Lordshill catchment No. 2

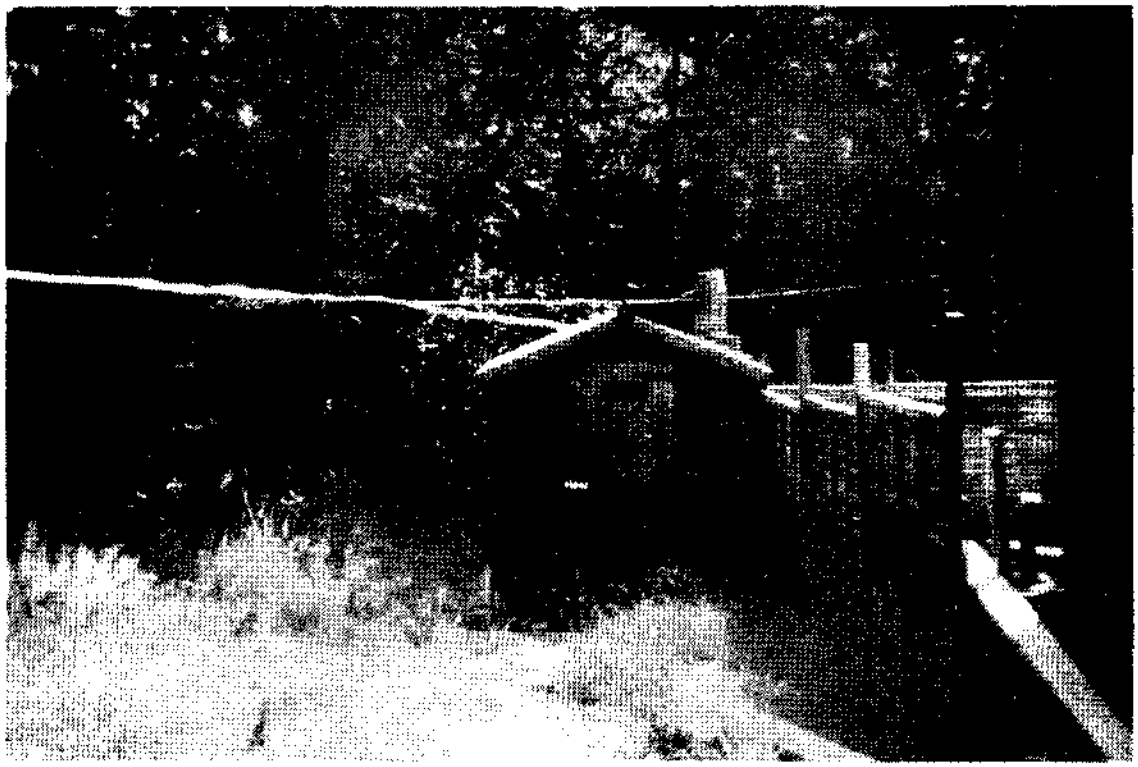

Figure 16: Instrumentation cabin

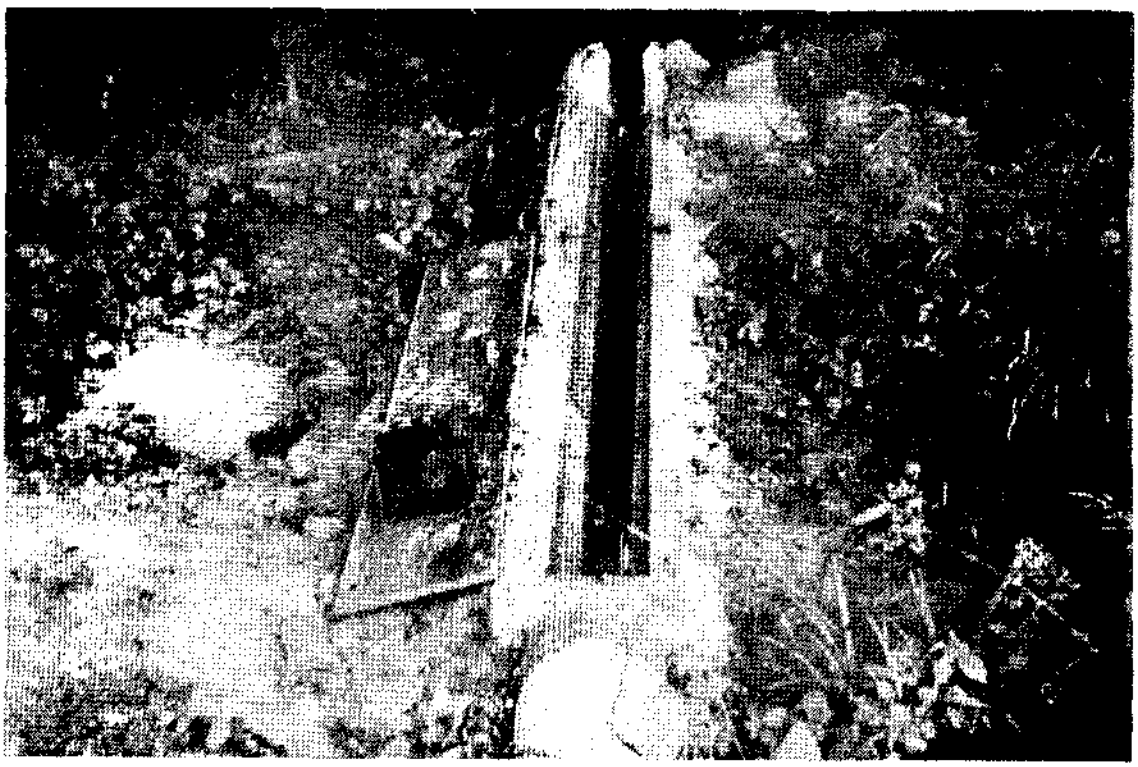

Figure 17: Channel and flume at outfall No. 2 (with covers removed)

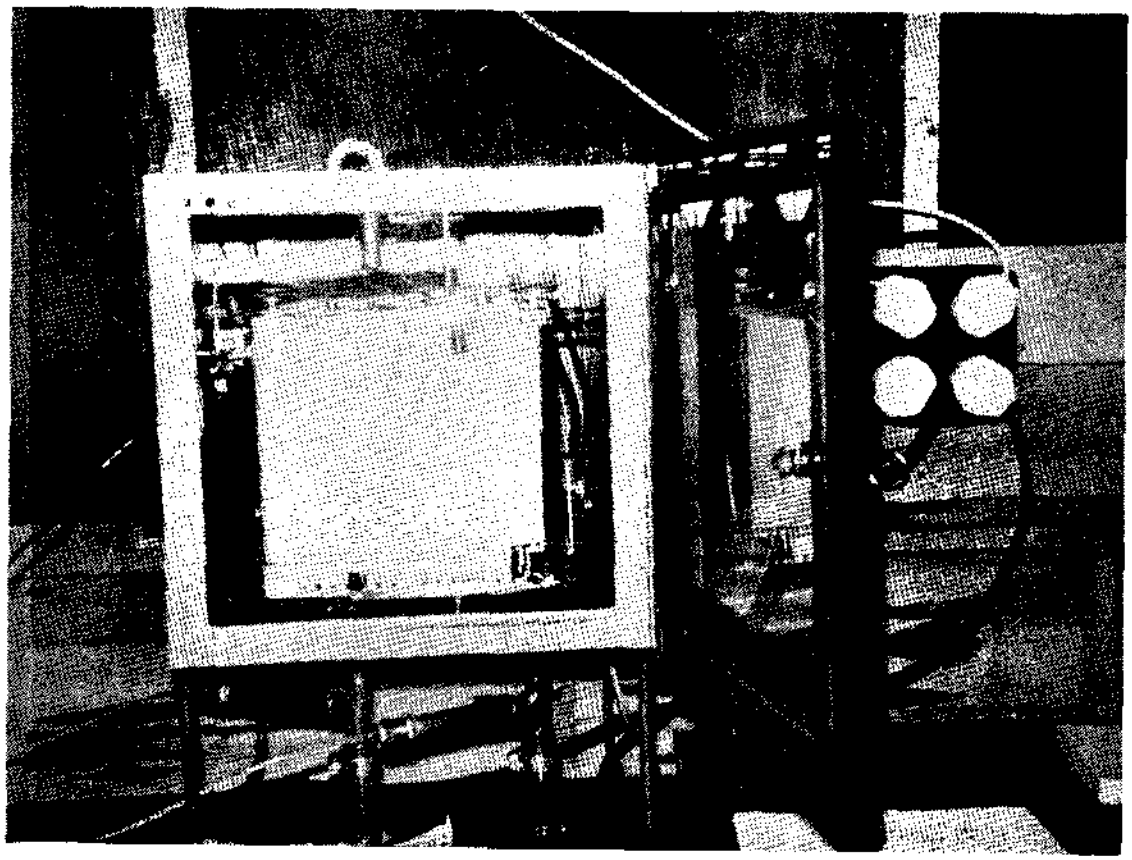

Figure 18: Arkon recorder

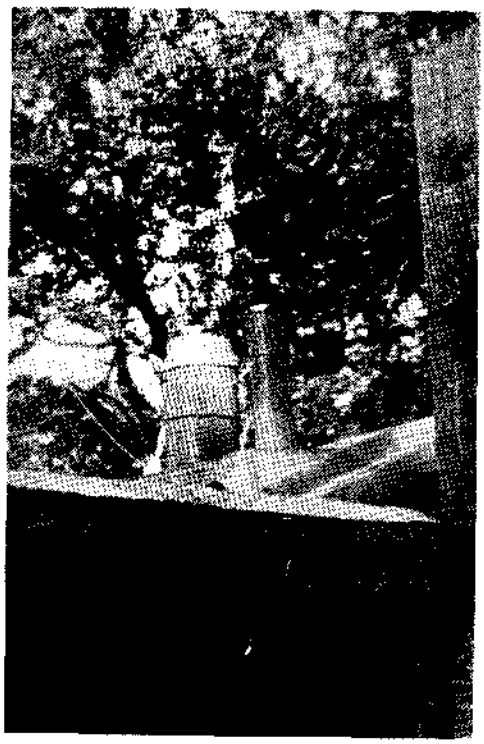

Figure 19: Raingauges 1 and 2

Figure 20: Raingauge 3

It is steeper than Catchment no. 1, with an average ground slope of 6.0%. Figure 15 is a view of Fulmar Close as seen from Sandpiper Road, the top limit of the catchment.

Catchment Data

A survey was undertaken to determine the required catchment data for use in the mathematical modelling part of the study. Some data relating to road widths and sewer pipes were available from original drawings, but these needed to be checked and augmented by an extensive field survey. The results of this survey are shown in Tables 1 and 2 which refer to the catchment data for Lordshill catchment numbers 1 and 2 respectively. Type 1 area refers to pavement and type 2 area to roof. Where the figure 99 appears in the column marked "junction above", this refers to a remote inlet.

Runoff Gauging

The runoff from the two catchments was monitored at their respective outfalls using Venturi flumes. The outfall installations were identical in all but one detail, and therefore only one will be described. The company responsible for the construction of the estate fortunately neglected to erect an outfall structure and had left the 229 m outfall pipe about 3 metres short of the brook. This length was employed to advantage in the installation of the flume.

The Venturi flume, supplied by Arkon instruments of Cheltenham, is made of precast glass fibre and is of U-section, going from 229 mm normal width to 152 mm throat width. A 300 mm square precast stilling-basin was connected at a position 457 mm upstream of the Venturi throat. A length of 229 mm wide U-section channel was constructed out of glass-fibre in the Southampton University workshops. This channel was connected, prior to installation, to the end of the Venturi flume, in order to provide sufficient upstream distance for undue turbulence to subside. (The length of channel is 1.8 m and 2.7 m for outfall nos. 1 and 2 respectively, and depended on the available distance between outfall pipe and brook). The structure was installed by connecting the upstream end to the outfall pipe, levelling it through its length, and setting it in concrete in situ. The structure was then covered with ¾" marine-ply boards (fixed with set screws and captive nuts for convenient removal) to protect it from vandalism. Figure 17 shows the gauging structure at outfall no. 2, with the channel and flume boards removed, but with the stilling-basin board in place.

It was realized after measurement had been in progress for about three months that the flow in the approach channel at outfall no. 2 was supercritical, causing the flow to "shoot" through the flume without attaining the subcritical condition necessary for its correct operation. To correct this fault, an energy dissipator was incorporated close to the upstream end of the approach channel to force the flow to attain its necessary subcritical regime. It was attached to the underside

Lordshill Catchment no. 1

PIPE NO.	JUNCTION NO.	JUNCTION ABOVE	DIAMETER (m)	SLOPE (%)	LENGTH (m)	TYPE 1 AREA (m^2)	TYPE 2 AREA (m^2)
1	1	99	0.00	0.00	0	210	0
2	2	99	0.00	0.00	0	0	133
3	3	99	0.00	0.00	0	0	133
4	4	99	0.00	0.00	0	90	266
5	5	99	0.00	0.00	0	0	150
6	6	1	0.15	4.00	38.1	640	0
7	7	5	0.10	5.20	14.0	97	0
8	7	6	0.15	4.76	25.0	0	0
9	8	3	0.10	6.50	14.0	203	0
10	8	7	0.15	2.70	34.7	0	0
11	9	4	0.15	0.95	21.0	44	200
12	10	9	0.15	0.95	32.0	240	200
13	11	8	0.23	2.44	18.7	692	0
14	12	2	0.10	8.10	16.5	0	0
15	12	10	0.15	0.95	20.0	0	0
16	12	11	0.23	2.44	18.7	0	0
17	13	12	0.23	0.48	33.5	0	0
					TOTALS	2216	1082

Average ground slope = 3.0%

Table 1: *Catchment data for Lordshill catchment No. 1*

Lordshill Catchment no. 2

PIPE NO.	JUNCTION NO.	JUNCTION ABOVE	DIAMETER (m)	SLOPE (%)	LENGTH (m)	TYPE 1 AREA (m^2)	TYPE 2 AREA (m^2)
1	1	99	0.00	0.00	0	509	0
2	2	99	0.00	0.00	0	34	200
3	3	99	0.00	0.00	0	15	200
4	4	2	0.10	6.95	16.8	22	133
5	5	3	0.10	5.89	21.3	32	200
6	6	4	0.10	3.05	27.4	57	200
7	7	5	0.10	5.89	22.3	70	200
8	8	1	0.15	7.69	14.6	477	0
9	8	6	0.15	3.05	16.8	0	0
10	9	7	0.15	4.27	32.3	41	133
11	10	8	0.15	4.76	35.4	0	0
12	10	9	0.15	4.27	7.0	0	0
13	11	10	0.23	5.00	24.4	0	0

Average catchment slope = 6.0%

Table 2: Catchment data for Lordshill catchment No. 2

of the channel's protective board, and may be seen in Figure 17. Outfall no. 1 differs from the other only in that it has no energy dissipator and has a shorter length of approach channel. However, this configuration is satisfactory since the approach flow to outfall no. 1 is subcritical.

The water-level in the stilling-basin is monitored using an Arkon Instruments air-purge system. A dip-tube in the stilling-basin is connected to the Arkon instrument, which is housed in the instrumentation cabin, by a length of 19 mm ID flexible nylon tubing. An HI-FLO miniature air compressor is connected into this tube by a T-junction situated immediately beneath the Arkon Instrument. Air is pumped continuously into the system and bubbles out of the dip-tube. The water-level in the stilling-basin is sensed at the instrument as an air pressure, which is converted by a pressure transducer and output as a pen-recording of water-level on a moving chart.

Both outfall flume water-levels are monitored in this fashion, resulting in simultaneous traces on the Arkon chart. The chart is driven by a mains AC motor at a speed of three inches/hour. Figure 18 shows the Arkon instrument with the two water-level pens at the bottom right of the chart (one is a red-ink trace and the other blue, to avoid confusion) and the raingauge extension pen at the top of the chart (see page). The conversion of water-level to discharge was achieved by a stage-discharge relation, validated by subsequent field calibration (see Figure 21 and Table 3).

Rainfall Gauging

The rainfall is monitored using three gauges, the locations of which are shown in Figure 13. Gauge No. 1 is a Casella Tipping Bucket Raingauge (W5698) and is located on the roof of the instrumentation cabin. Each tilt of the bucket is registered inside the cabin on a Casella Receiver (W5705), the solenoid for which is operated by a 6-volt battery. The receiver chart moves at a speed of 12 inches/day.

A connection was rigged up between the Casella and the Arkon instruments. The mechanical action of the rainfall recorder triggers a microswitch in a mains AC circuit, which, in its turn, activates another solenoid mounted on the Arkon instrument. The mechanical action of this solenoid leaves a small mark on an otherwise continuous trace on the Arkon chart. The benefits of this extension are two-fold; firstly, it enables the rainfall/runoff items to be synchronised; and, secondly it provides more sensitive definition of higher rainfall intensities by virtue of the greater speed of the Arkon chart drive.

Gauge No. 2 is a Casella Snowdon Standard Rainguage, and is sited next to the tilting bucket gauge on the cabin roof as a check on the latter's performance. Figure 19 shows raingauges 1 and 2 attached to a level platform on the roof. The disadvantage of the position of

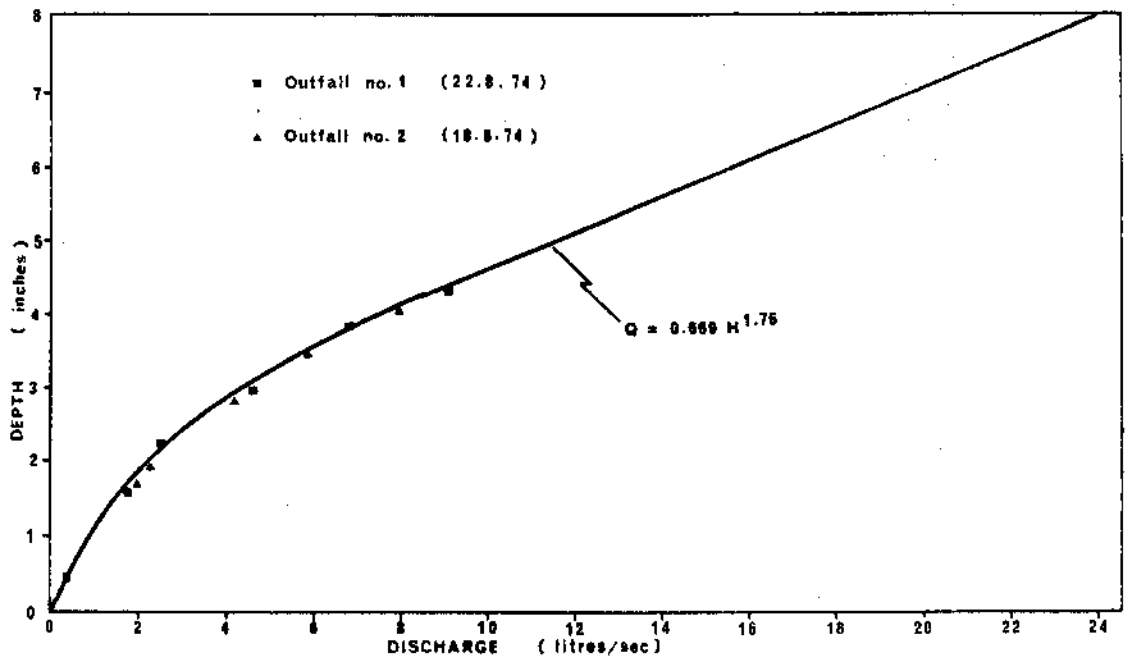

Figure 21: Stage discharge relation for 9" Venturi flume

Test No.	Location	Flume depth (inches)	Vol. collected (gals)	Time (secs)	Discharge (litres/s)	Est. error (%)
1	outfall no. 1	1.46	15.0	50.2	1.36	4
2	outfall no. 1	2.19	32.5	60.0	2.46	3
3	outfall no. 1	2.90	36.5	35.8	4.63	4
4	outfall no. 1	3.80	42.5	28.0	6.91	4
5	outfall no. 1	4.21	34.5	18.9	9.01	5
6	outfall no. 2	0.52	10.0	149.3	0.30	5
7	outfall no. 2	1.52	29.0	81.3	1.62	3
8	outfall no. 2	1.84	37.5	76.0	2.25	2
9	outfall no. 2	2.67	38.2	42.2	4.11	2
10	outfall no. 2	3.32	35.8	27.0	6.02	3
11	outfall no. 2	3.99	37.8	21.8	7.89	5

Table 3: Field calibration tests

these two gauges is that the site does not conform on two counts to the British Standard recommendations for the positioning of raingauges.

Firstly, the rims are not the regulation 300 m above ground level, and, secondly, the distance from the nearest obstruction (in this case, the tree canopy) is about ¾ times the obstruction's height instead of the regulation two times. The advantages of the position are, firstly, that the tipping bucket gauge may be conveniently connected to its recorder, and secondly, but most importantly, that the site is relatively vandal-proof.

Gauge No. 3, as shown in Figure 20, is a Casella Snowdon Standard Raingauge. It is sited in a position which conforms with British Standard recommendations. Owing to its correct siting, it is employed as the reference gauge, and the tipping bucket gauge is used to distribute temporally the total rainfall depths measured by the former. It has been found that, in general, the roof gauges tend to catch less than gauge No. 3. Table 4 shows this discrepancy, and the rainfall intensities calculated from the tipping bucket gauge were multiplied by the error value indicated in the right hand column of Table 4 to give the true rainfall intensities.

TIME INTERVAL	STORM NUMBERS	TOTAL VOLUME COLLECTED (mm) GAUGE 1 (TIPPING BUCKET)	GAUGE 2 (ROOF STANDARD)	GAUGE 3 (GROUND STANDARD)	PERCENTAGE ERROR (+ve=GDVOL >TBVOL)
16/6 - 17/ 6/74	1	14.0	20.0	not sited	-
17/6 - 18/ 6/74	2	4.0	3.9	4.2	+ 5.00
25/6 - 26/ 6/74	3	20.0	20.6	20.5	+ 2.50
26/6 - 28/ 6/74	4	39.5	42.6	44.6	+ 12.91
28/6 - 1/ 7/74	5	7.5	7.4	7.8	+ 4.00
5/7 - 18/ 7/74	6	34.5	34.5	37.8	+ 9.56
8/8 - 10/ 8/74	7	5.5	5.3	5.8	+ 5.45
10/8 - 14/ 8/74	8	13.0	15.4	13.4	+ 3.07
26/8 - 27/ 8/74	9	22.0	22.5	23.6	+ 7.27
29/8 - 2/ 9/74	10,11,12	28.5	28.6	31.2	+ 9.47
2/9 - 3/ 9/74	13	9.0	8.5	9.5	+ 5.55
21/9 - 23/ 9/74	14	16.5	16.6	18.7	+ 13.33
23/9 - 24/ 9/74	15	9.0	9.4	9.6	+ 6.67
30/9 - 3/10/74	16	4.0	4.0	4.1	+ 2.50
17/6 - 19/ 6/75	17	21.0	21.8	22.0	+ 4.76
8/7 - 9/ 7/75	18	12.0	12.5	12.6	+ 5.00
4/8 - 5/ 8/75	19	6.6	6.8	7.2	+ 10.76

$$\text{percentage error} = \left(\frac{GDVOL}{TBVOL} - 1\right) * 100$$

Table 4: Total rainfall volumes from 3 raingauges

Collection and Preparation of Rainfall-Runoff Data

Rainfall and runoff records were obtained from the Casella (daily) and Arkon (weekly) charts for the periods June to December 1974 and March to August 1975, from which isolated storm events were selected. The selection criterion was a subjective one, being all events causing a peak depth of flow of more than 75 mm in either flume stilling-basin (equivalent to an approximate discharge of 5 litres/s). The water-level records were converted to discharge, the complete digitising of the raw data being done by hand.

Some of the storm events recorded unfortunately had to be rejected. The first significant event (Storm No. 1, 16/6/75) was rejected because of unreliable rainfall data. Raingauge No. 3 had not been installed at this date, and the two roof raingauges recorded an inexplicable difference in their measurement of total rainfall depth.

The only other malfunction of the rainfall gauging system occurred in July 1974 when a blockage in the tilting bucket raingauge caused it to underread. However, no significant storm events were lost due to this malfunction.

The major cause of data loss was the surcharging of the sewer outfalls. Under circumstances where there had been a lot of antecedent rainfall, a heavy rainstorm would cause the water-level in the brook to rise swiftly and drown the flumes, causing the runoff traces to be obscured. A number of major events were lost in this fashion, and these events do not appear in the reduced list of events. In general, the surcharging of the brook caused the runoff records on both flumes to be lost at approximately the same time. However, in the case of storm No. 17 (see Table 5), it proved possible to retrieve most of the runoff from catchment No. 2 before its flume became surcharged. The missing portion of the recession limb for this hydrograph was artificially obtained from the recession limbs of other hydrographs. During 1975, the brook was kept clear of debris in an attempt to eliminate the surcharging, without complete success. It might be possible to reduce or eliminate the effects of surcharging by improving or diverting the brook.

The runoff records for storms 2 to 6 on catchment No. 2 were unreliable due to supercritical conditions in the approach channel, as discussed under the Runoff Gauging heading. For this reason, events 2 to 6 were only used for analysis on catchment No. 1.

With the exception of those mentioned in the above three paragraphs, all suitable and significant storm events were reduced to a form suitable for computer analysis. Table 5 gives a list of these storms employed for analysis with brief details. A fuller description of the temporal distribution of the rainfall and runoff records may be found in Figures 30 to 59. The number of significant events is dependent on two factors: firstly, the criterion for significance; and, secondly, the frequency of occurrence of such events in any given year. Bearing in mind the first of these factors and the number of events lost to surcharging, it is the opinion of the author that, during the summer of 1974, Southampton had more than its normal share of heavy rainfall events.

				CATCHMENT NO. 1			CATCHMENT NO. 2	
STORM NUMBER	DATE	ANTECEDENT CONDITIONS	DURATION (minutes)	RAINFALL VOL.(mm)	RUNOFF VOL. (mm)	RAINFALL/RUNOFF PERCENTAGE	RUNOFF VOL. (mm)	RAINFALL/RUNOFF PERCENTAGE
2	17/6/74	DRY	33	4.18	3.14	75.1		
3	26/6/74	DRY	79	8.40	4.87	57.9		
4	27/6/74	DRY	25	3.69	2.27	61.5		
5	1/7/74	DRY	62	6.47	3.91	60.4		
6	14/7/74	DRY	51	4.73	2.34	49.4		
7	9/8/74	DRY	15	2.21	1.88	85.0	1.41	63.7
8	12/8/74	WET	27	3.18	3.38	106.4	2.11	66.3
9	26/8/74	WET	96	9.69	9.13	94.3	6.75	69.7
10	30/8/74	WET	18	3.74	2.28	61.4	2.02	54.4
11	31/8/74	WET	75	9.97	9.62	96.5	6.95	69.8
12	2/9/74	WET	51	8.13	10.04	123.5	6.04	74.3
13	2/9/74	WET	17	4.12	5.11	124.1	3.32	80.6
14	21/9/74	WET	17	3.12	2.25	72.2	2.26	72.3
15	23/9/74	WET	9	4.52	4.39	97.1	3.55	78.4
16	3/10/74	DRY	6	2.00	1.26	63.0	1.28	64.0
17	12/6/75	WET	23	11.52			7.80	67.7
18	8/7/75	DRY	9	4.72	2.47	52.3	3.11	66.0
19	5/8/75	WET	9	2.34	1.25	53.4	1.50	63.9

Table 5: Storms used for analysis

IV : APPLICATION OF THE MODEL

It is first necessary to evaluate the parameters (of which there are eight in the non-linear reservoir case). Where possible parameters are assessed from physical considerations; alternatively, parameters may be evaluated either by intuitive judgements or by some optimisation procedure. It would be possible to release all parameters and subject them to some automatic optimisation routine. However, as will be discussed at a later point, it was considered that the difficulties of selecting representative objective functions and of interpreting the meanings of optimised solutions would render such an optimisation exercise of little value. In the event, only two of the parameters were subjected to an optimisation procedure, the remainder were estimated in other ways, as are discussed below.

Parameter estimation by physical considerations

DEPRESSION STORAGE: Since depression storage is the first submodel, then the parameters for this submodel will be dealt with first. As has been discussed in Section I, the depression storage is given by a depth of water which may be subtracted from the rainfall input before overland flow may be assumed to commence.

Work at John Hopkins University, Maryland, U.S.A. yielded results which allowed Veissman (1966) to give a tentative relationship between depression storage and catchment slope, as follows:-

$$DS = 3.30 - .765 \times SLOPE \qquad \ldots (4.1)$$

where DS is the depression storage (mm)

and SLOPE is the average catchment slope (%)

The above expression was derived from results obtained from work done mainly on short lengths of road and parking lots, and is given for slopes between 1% and 3%. Willeke (1966) found a very similar relationship from the same data set. While the relationship is understood as tentative, it gives a guide to the order of magnitude of the size of the depression storage parameter for the paved area. For Lordshill catchment number 1, the depression storage is taken from equation 4.1 as 1.0 mm. The average catchment slope for catchment number 2 falls outside the range of equation 4.1, and thus an intuitive judgement was made to give a value of 0.75 mm.

In the case of the roofed surfaces, no indication of the value of depression storage was found. It was considered that the filling of surface depressions was no longer applicable, and that depression storage was in this case synonymous with surface wetting. Another

intuitive judgement gave a value of 0.1 mm for the depression storage for the roofed areas in both catchments, and it may be noted that such a depth is a very small proportion of the total rainfall volume and is likely to have little effect on the output hydrograph.

In many cases, a storm occurred within a longer rainfall event or very shortly after another event. In such circumstances, depression storage was taken to be satisfied.

PERCENTAGE RUNOFF: The value of the percentage runoff parameter is a function of so many different variables that to attempt an evaluation on physical grounds would prove impracticable. The nature of this particular problem lends itself well to a statistical approach, where a large quantity of data may be employed to produce a regression predicting the percentage runoff on pertinent variables, such as some catchment wetness index, catchment slope, volume of rainfall, etc. Such an approach would allow an engineer to predict the percentage runoff where no data were available for a particular catchment.

In the case of this particular study, the measured outfall volume was employed to compute the percentage runoff. In this manner, the predicted outfall volume was effectively "forced". This procedure may be construed as using the result to prove the result, but this argument would only apply where the object of the study was to predict the percentage runoff. The object in fact is to demonstrate the viability of the non-linear reservoir submodel for surface routing, and, as such, the "forcing" procedure recommended here assists in this demonstration.

OTHER PARAMETERS: A value of Manning's n is taken for the pipe routing part of the model as 0.013. This is a text-book value for flow in a partially-full concrete pipe. For a large catchment, the model output is found to be relatively sensitive to the value of Manning's n, but it is likely that, for catchments of the size of those employed in this study, the model is relatively insensitive to variation in this value.

A quasi-physical justification for the value of the non-linearity parameter of the non-linear surface routing submodel was given in Section I for paved surfaces. The same value was given to the non-linearity parameter for the roofed surfaces. While the same physical justification does not apply in this case due to the inapplicability of Chezy's formula to such a flow regime it is considered that approximately the same degree of non-linearity is likely to occur in this case as for paved surfaces.

The remaining parameters, for which there may be no physical or intuitive assessment, are the routing constants, K_1 and K_2 (corresponding to paved and roofed areas respectively), for the surface submodel. For these, an optimisation procedure was employed as explained below, not only to determine their optimum values but also to investigate the variation of these optimum values from event to event and the effect which this variation has on any given event.

The optimisation of the surface routing constants for non-linear model

The initial difficulty with any optimisation problem lies in the choice of objective function. It is somewhat paradoxical that this initial choosing of the objective function should itself be such a subjective process. The objective function provides a quantitative measure of the goodness of fit between measured and modelled output. In some instances, it is possible to achieve such a quantitative measure which matches well the criteria which define the goodness of fit. In other circumstances, these criteria are so diverse that such a commonly suitable objective function may not be apparent, and it seems that the case in question is just such a circumstance. It was found that when various different objective functions were employed, corresponding to different criteria for goodness of fit, different optimum values of K_1 and K_2 for different objective functions were obtained. It was decided to generate optimum values of K_1 and K_2 corresponding to four different objective functions, and then to consider these pairs of values subjectively to give an overall optimum pair of values. The four objective functions employed are as follows:

1. Peak value
2. Time to peak
3. Direct least squares fit
4. Biassed least squares fit

The first two are self-explanatory, representing the objective function which gives the values of K_1 and K_2 producing the best prediction of peak value and of time to peak. The third objective function is the standard least squares fit, as illustrated in Figure 22. The error at time t is given by

$$\varepsilon_t = Q_{MOD_t} - Q_{OBS_t} \qquad \ldots (4.2)$$

and the goodness of fit is represented by the Integral Square Error, given by

$$ISE = \left| \sum_{t=\frac{1}{2}}^{N} (\varepsilon_t)^2 \right|^{\frac{1}{2}} / \sum_{t=1}^{N} (Q_{OBS_t}) \times 100\% \qquad \ldots (4.3)$$

The above criterion for goodness of fit is a popular one, and gives no direct weighting to any particular region of the hydrograph.

It was felt that this objective function has its drawbacks for the optimisation of single events, and thus a further objective function was devised. If the circled area of Figure 22 is expanded, we get Figure 23. From this, we can see that AD might perhaps be a better indication of the error ε_t at time t than AC, as used in equation 4.2 above. AD may be calculated from

$$AD = AC/\sqrt{1 + (AC/AB)^2} \qquad \ldots (4.4)$$

By applying ε_t = AD to equation 4.3, we get effectively a biassed value of ISE, as indicated by the fourth objective function in the above list. Its major drawback lies in the conflict of units between the distances AC (litres/s) and AB (minutes). Some subjective evaluation is required of the relative importance of the two units and it has been found that different optimum pair values can be obtained by using different conversion ratios for the conflicting units. The drawbacks and implications of the use of the biassed least squares fit as an objective function only became apparent as it was being employed, and it is clear that it leaves much to be desired. However, results incorporating it are included, with due consideration given to its limitations.

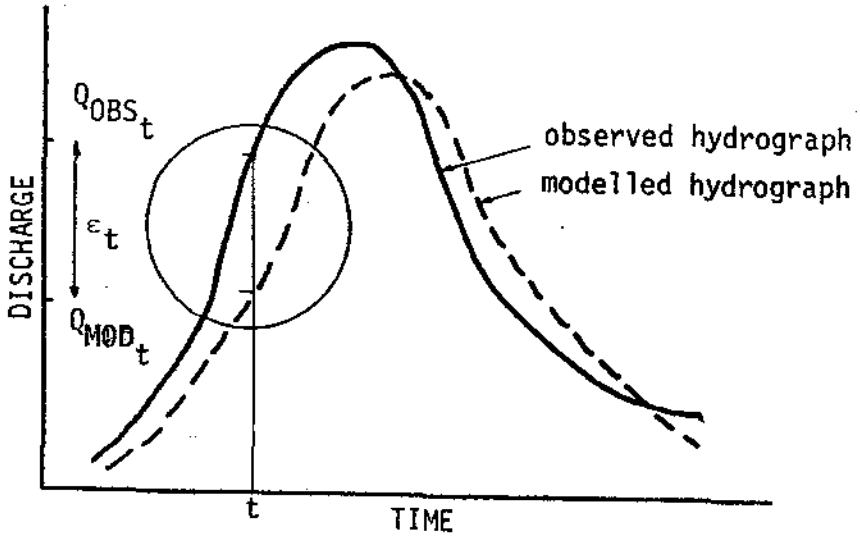

Figure 22: Direct least squares fit

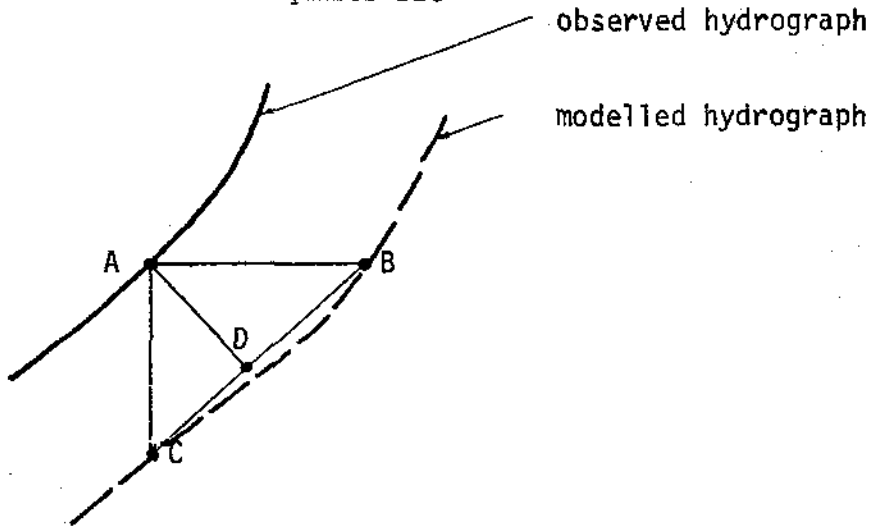

Figure 23: Expanded view of Figure 22

Figure 24 shows the response surfaces for two goodness of fit objective functions for one storm. It will be noted that the axes of the plot are K_1 and the ratio K_1/K_2. It may be argued that the two axes are dependent, but the counter to that is that K_1 and K_2 are themselves dependent and that an equal dependency would exist for a plot of K_1 against K_2. The plot shows that the response surface is well behaved, with no readily apparent local minima. As in all cases studied, there is a "valley" with its axis in the direction of the K_1/K_2 axis or with a slight slope in the + K_1 direction. This would indicate that the objective function is much more sensitive to the value of K_1 than to the ratio K_1/K_2, which in turn indicates a relative lack of sensitivity to the roofed area routing constant, K_2. This latter fact is to be expected, since the response from roofed areas would appear to have, from consideration of likely times of travel, a much smaller lag time than the response from paved areas. This valley tendency was found consistently for all the storms studied.

In some cases, the four objective functions produced a compatible pair of value for the parameters, in which case there was no problem in choosing one representative pair of values of K_1 and the ratio K_1/K_2. In most cases, however, some subjective judgement was necessary in the choosing of the optimum pair of values. As a procedure, the peak value and time to peak were taken as the most important objective functions and the third and fourth were considered as weighting functions. Table 6 shows the optimised values of K_1 and the ratio K_1/K_2 for the four objective functions together with the optimum pair of values assessed subjectively for each storm on Lordshill catchment number 1, while Table 7 demonstrates the same for Lordshill catchment number 2. The average value of the constants K_1 and K_1/K_2 are also given for each catchment.

Tables 6 and 7 demonstrate that the optimum routing constants vary quite considerably from storm to storm for a given catchment. However, no trend is immediately noticeable to indicate that the optimised values are related to storm characteristics. Optimum values of K_1 vary from 20.0 to 33.0 for Lordshill catchment number 1, and between 15.0 and 33.0 for catchment number 2. However, it is found that there is no very significant difference between the modelled hydrographs with individually optimised parameters and with overall average parameters, as demonstrated for one storm in Figure 25.

What is a little more surprising is that the average values of K_1 and the ratio K_1/K_2 are very similar for the two catchments. It was expected that there would be a very definite correlation between average catchment slope and the optimum routing constants. However, while Lordshill catchment number 1 is of a somewhat milder slope than catchment number 2, they are both relatively steep and different values of the parameters may be necessary for flatter catchments.

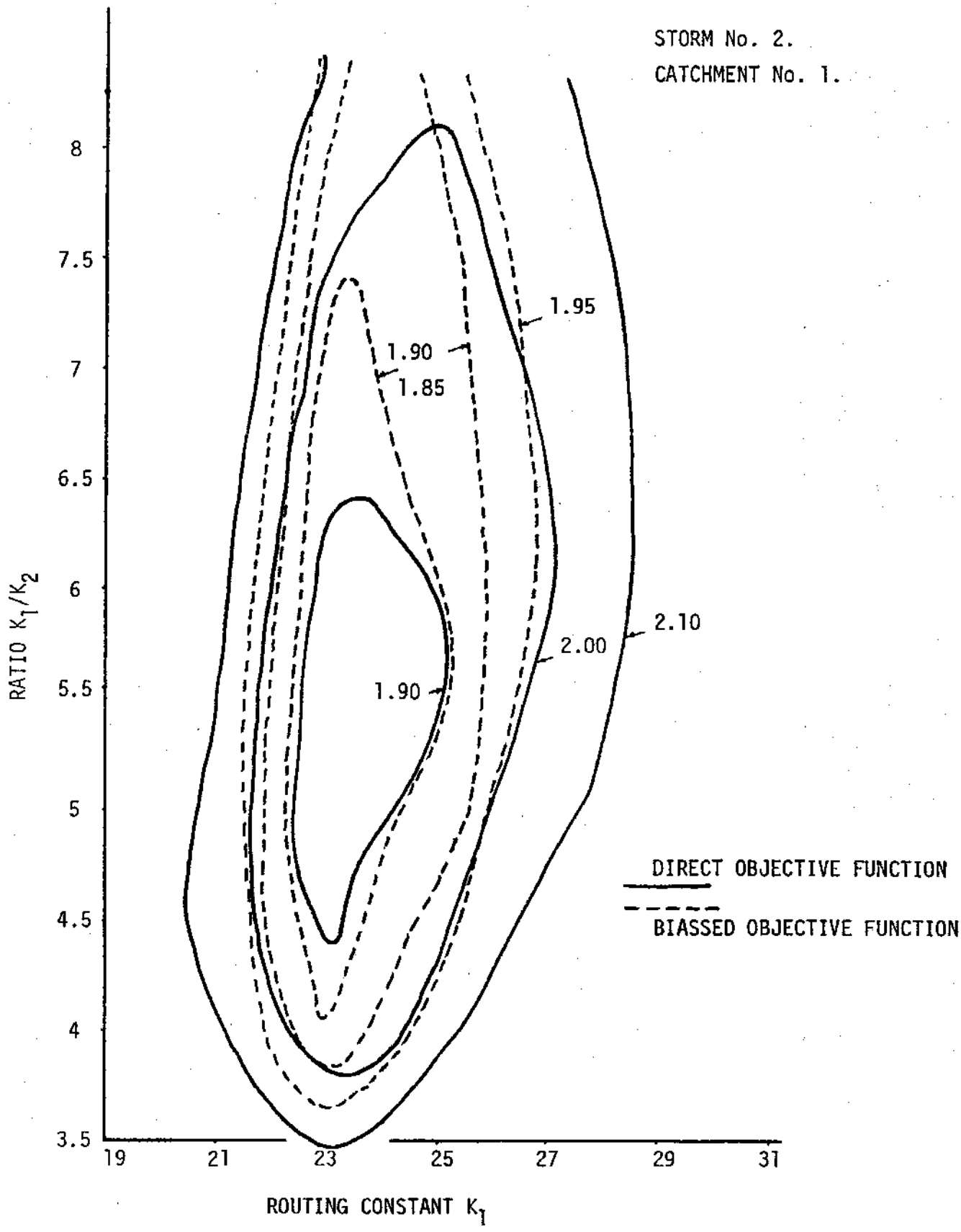

Figure 24: Response surfaces of optimisation exercise

STORM No.	PARAMETER	PEAK VALUE (L/S)	TIME TO PEAK (mins)	DIRECT O.F.	BIASSED O.F.	"OPTIMUM" VALUES
2	K_1	21.0	any	23.0	23.0	22.0
	K_1/K_2	any	any	5.2	5.2	5.0
3	K_1	33.0	any	33.0	33.0	33.0
	$K_1K/_2$	any	any	3.5	3.5	3.5
4	K_1	25.0	any	31.0	27.0	25.0
	K_1/K_2	any	any	3.5	3.5	3.5
5	K_1	23.0	any	30.0	32.0	25.0
	K_1/K_2	low	any	3.5	3.5	3.5
6	K_1	29.0	25.0	33.0	33.0	31.0
	K_1/K_2	low	low	3.5	3.5	3.5
7	K_1	30.0	any	29.0	29.0	31.0
	K_1/K_2	5.0	any	9.0	9.0	7.o
8	K_1	No realistic best fit possible				- - -
	K_1/K_2					- - -
9	K_1	23.0	low	31.0	31.0	23.0
	K_1/K_2	any	any	5.5	5.5	5.5
10	K_1	19.5	any	21.0	21.0	20.0
	K_1/K_2	any	mid range	4.5	3.5	5.0
11	K_1	30.0→33.0	any	32.0	31.0	31.5
	K_1/K_2	5.0	any	any	any	5.0
12	K_1	15.0→21.0	21.0→	23.0	23.0	21.0
	K_1/K_2	low	any	6.5	7.5	6.0
14	K_1	21.0	any	21.0	23.5	21.0
	K_1/K_2	5.0	high	9.0	9.0	6.0
15	K_1	25.0	any	25.1	23.0	25.0
	K_1/K_2	any	low	5.1	7.0	5.0

Average "optimum" K_1 = 25.7 (S.D. 4.5)
Average "optimum" K_1/K_2 = 4.9 (S.D. 1.1)

Table 6: Optimum parameter values (K_1 and K_2) for Lordshill catchment Number 1.

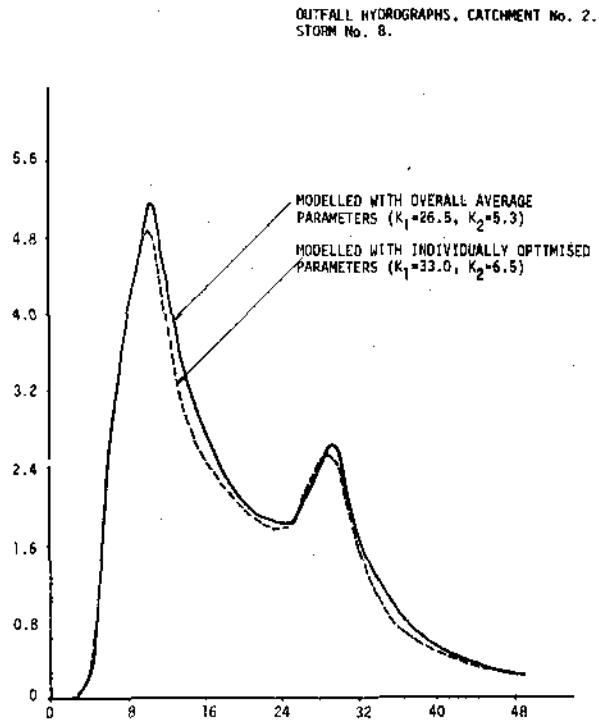

Figure 25: Effect of using overall average parameters

STORM No.	PARAMETER	PEAK VALUE (L/S)	TIME TO PEAK (mins)	DIRECT O.F.	BIASSED O.F.	"OPTIMUM" VALUES
7	K_1	33.0*	any	33.0	33.0	33.0
	K_1/K_2	6.0	any	7.0	7.0	6.0
8	K_1	33.0	any	33.0	33.0	33.0
	K_1/K_2	5.0	high	3.5	3.5	5.0
9	K_1	15.0	15.0	33.0	33.0	15.0
	K_1/K_2	any	any	3.5	3.5	3.5
10	K_1	33.0	23.0-33.0	33.0	33.0	33.0
	K_1/K_2	3.5	4.5	4.5	4.5	3.5
11	K_1	18.0	15.0-19.0	any	any	18.0
	K_1/K_2	6.0	high	any	any	6.0
12	K_1	25.0	any	any	any	25.0
	K_1/K_2	any	low	any	any	4.5
14	K_1	28.0*	any	any	21.0	28.0
	K_1/K_2	8.0	any	9.0	9.0	8.0
15	K_1	27.0*	any	33.0	33.0	27.0
	K_1/K_2	5.55	high	5.0	7.0	5.55

Average "optimum" K_1 = 26.5 (S.D. 6.6)
Average "optimum" K_1/K_2 = 5.3 (S.D. 1.4)

* Other pair values also available

Table 7: Optimum parameter values (K_1 and K_2) for Lordshill catchment Number 2.

The optimisation of the routing constants for the linear reservoir

Some attempt was made to optimise the routing constants for the linear case. However, for all but a few of the storms, it was found that the four objective functions were generally incompatible. In the majority of cases, it was not possible to reproduce the peak value either at a realistic time to peak or for low value of the third or fourth objective function. Due to this fact, no extensive optimisation was attempted of the type used for the non-linear case. The values of 6.5 and 1.5 minutes for K_1 and K_2 respectively were those values which gave good results for Storms 3, 9, 12 and 14 for Lordshill catchment number 1 and for Storms 9 and 11 for catchment number 2.

Table 8 shows the values of the parameters applied to the model when used on the storms recorded for the Lordshill catchments.

PARAMETER	PARAMETER VALUES	
	LORDSHILL CATCHMENT 1	LORDSHILL CATCHMENT 2
Depression Storage (Roofs)	.10 mm	.10 mm
Depression Storage (Paved Areas)	1.00 mm	.75 mm
Percentage Runoff (Paved Areas Only)	forced	forced
Non-linearity Parameter (Roofs)	.67	.67
" " (Paved Areas)	.67	.67
Non-linear routing constant (Roofs)	25.7	26.5
" " (Paved Areas)	5.2	5.3
Linear routing constant (Roofs)	1.3	1.3
" " (Paved Areas)	6.5	6.5
Manning's n for pipeflow	.013	.013

Table 8 Parameter values for model demonstration

The sensitivity of the model parameters

It is the intention at this stage to study the sensitivity of the model to variations in the model parameters. To achieve this, the model was applied to Lordshill catchment number 1 using measured rainfall inputs but without recourse to a comparison of the modelled response with observed response. In this manner, it is hoped that the sensitivity of the model to each of its parameters will become apparent.

DEPRESSION STORAGE: The effect of the variation of the depression storage parameter is demonstrated in Figure 26 which shows three hydrographs modelled from storm No. 8, one including depression storage for both surface types, another including depression storage for paved surfaces only, and the third ignoring depression storage for both surface types. The model shows a definite sensitivity to the paved surface depression storage but appears relatively insensitive

to the roofed surface depression storage. This is to be expected, bearing in mind the relative magnitudes of the two parameters (1.0 mm for paved surfaces, 0.1 mm for roofed surfaces).

Storm No. 15, as demonstrated in Figure 26, shows a less accentuated dependency on depression storage than was found for storm No. 8. This is due to the difference in storm size. The depression storage parameters have a fixed value, while the rainfall volume alters greatly from storm to storm. Figure 26 would indicate that the model becomes less sensitive to the depression storage as the size of storm increases, as might be expected.

NON-LINEARITY PARAMETER n FOR SURFACE ROUTING : In order to demonstrate the sensitivity of the model to the surface routing non-linearity, it was necessary to vary also the routing constants, K_1 and K_2, in order that the lag times of the response might be the same. In the linear case, the routing constant is the response lag time (lag time is defined as the distance between the hydrograph centroids), but this

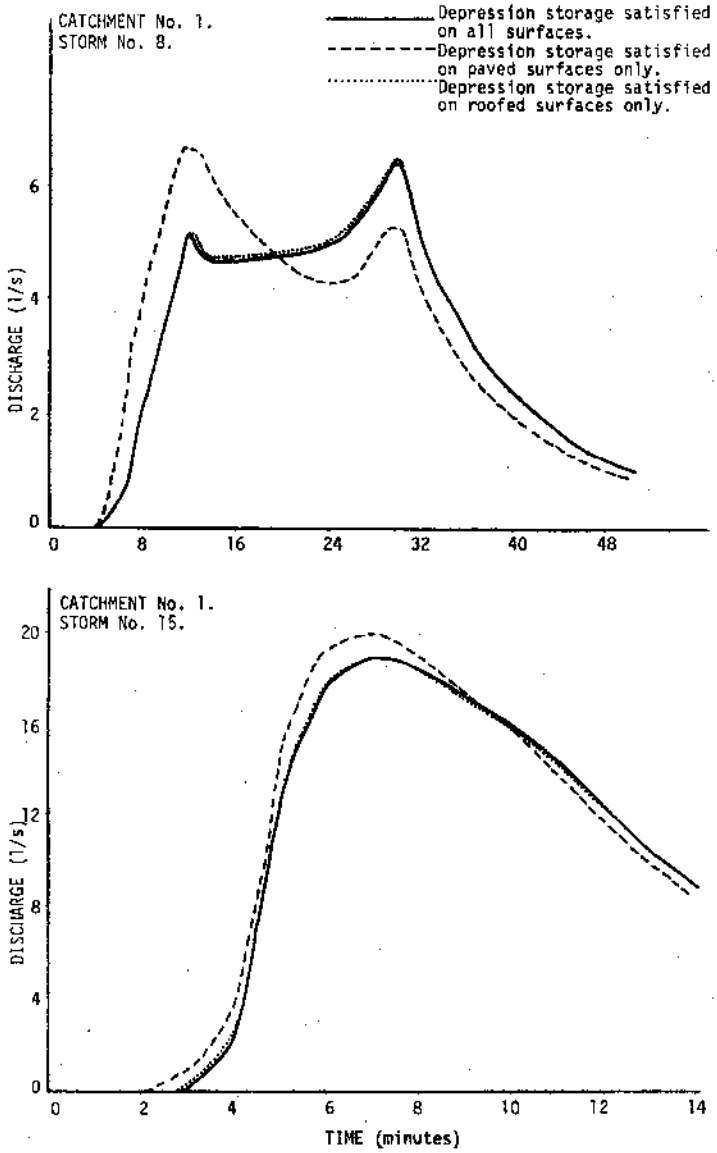

Figure 26: Effect of depression storage on model performance.

is not so in the non-linear case. Figure 27 shows the response hydrograph for three cases, for n = 1 (linear case), n = .67 (as used in the non-linear model) and n = .5 for storm No. 15. The corresponding routing constants, K_1 and K_2, are 6.5 and 1.3, 16.25 and 3.25, and 27.00 and 5.40 respectively. The linear case differs considerably from the two non-linear hydrographs, which themselves produce a fairly similar hydrograph. It is noticeable that, as expected, the linear hydrograph recedes much faster than its non-linear counterparts.

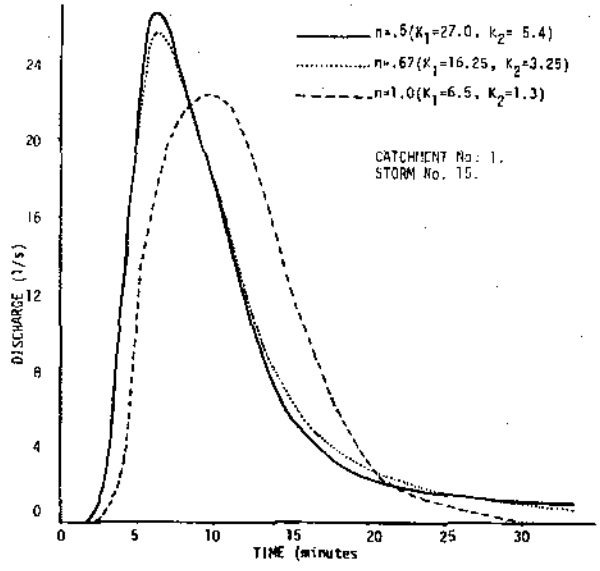

Figure 27: Effect of non-linearity n on model performance.

THE ROUTING CONSTANTS, K_1 and K_2: Figure 28 demonstrates the variation of the model output with the routing constants. The peak value decreases and time to peak increases for any increase in routing constant, as would be expected. Any percentage difference in roofed surface constant K_2 has a far smaller effect on hydrograph shape than the same percentage difference in paved surface constant K_1. This is consistent with the difference in magnitude of the response lag times, and appears to support the relative independence of the model on K_2 observed in the optimisation procedure earlier. The routing constants for the linear case will have a similar effect on the model output.

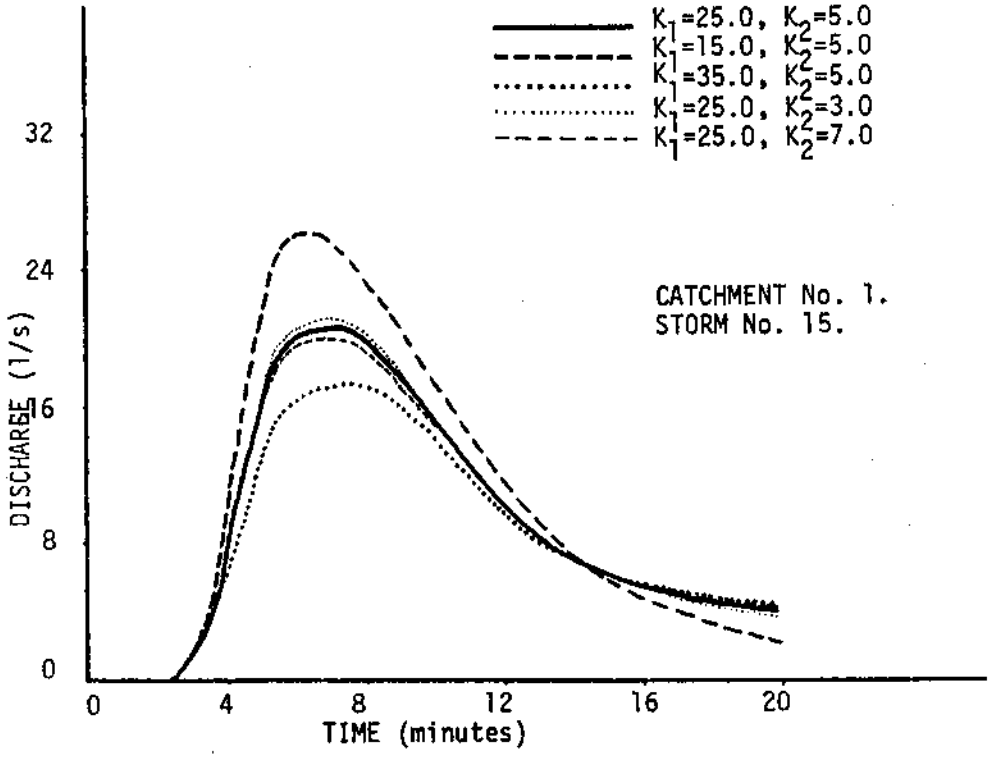

Figure 28: Effect of routing constants on model performance

MANNING's n FOR PIPEFLOW: Figure 29 demonstrates that the model is relatively insensitive to the value of Manning's n for the pipe routing part of the model. It is likely that the model would demonstrate greater sensitivity to this parameter for larger catchments, as observed by the author (1972) in a similar situation. Correspondingly, it is also possible that the model may become less sensitive to the surface routing constants as catchment size increases.

Comparison of the modelled output with observed output

The model was applied to the data collected on Lordshill catchment numbers 1 and 2, using the parameter values in Table 8. As explained in Section II, the model uses a kinematic pipe-routing method instead of the full characteristics method for high-energy situations. It was found that the minimum criterion for use of the kinematic method (Froude number greater than 2) was likely to occur on all storms in all but 3 pipes of catchment number 1 and in all pipes of catchment number 2. The model was run for one storm on catchment number 1 using the kinematic method on all pipes, and a negligible difference was observed between this model run and one using the full characteristics method for the 3 pipes where it was applicable. In order to save time and money in computing, the kinematic method was adopted in all cases.

Figures 30 to 46 demonstrate how the modelled hydrographs compare with the observed hydrographs for 17 storms on Lordshill catchment number 1. Figures 47 to 59 demonstrate the model for storms 7 to 19 on Lordshill catchment number 2. Storms 13, 16, 17, 18 and 19 are interesting for both catchments, as they have not been employed for the model optimisation. This was not intended as a

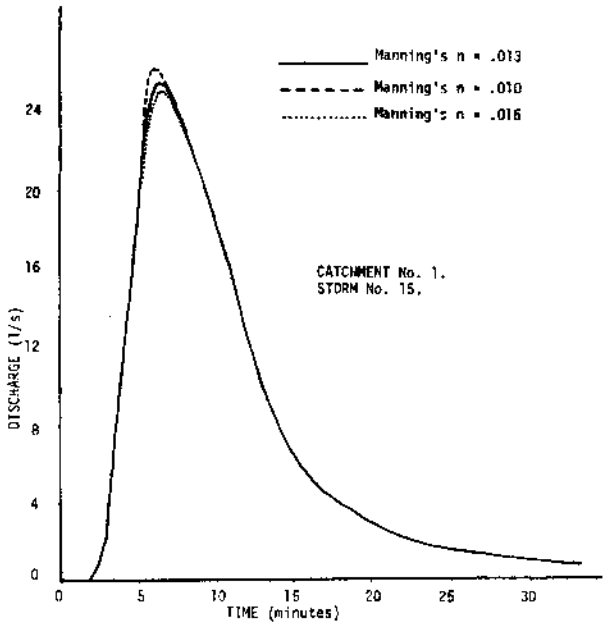

Figure 29: Effect of Manning's n on model performance.

split test study. The reason that these storms were not used in the optimisation was that they were not reduced for analysis at the time the optimisation was carried out. Certain general features may be gleaned from an examination of the model results.

The time of entry submodel consistently overestimates the value of peak runoff and the peak occurs consistently early. This value of peak could be forced to simulate the observed value, but the time of entry parameter value would be unrealistically large and the peak would occur much later than the observed peak. It is therefore concluded that the time of entry submodel cannot effectively simulate the inlet hydrograph. This last statement assumes a recognition that there is an appreciable change in shape between the rainfall excess and the inlet hydrograph.

The linear reservoir surface routing submodel allows for a certain change in shape between rainfall excess and inlet hydrograph. This fact is supported by the results, which demonstrate a much improved synthesis of observed hydrographs over the time of entry submodel. However, it may be seen that it is not possible in many cases to simulate both the peak value and the time to peak. As in the case of the time of entry submodel, the peak value in those cases where they do not already agree could be simulated, but the peak would then

occur at an unrealistic time. However, the disparity is not so exaggerated as in the time of entry case. The other notable feature of the linear simulation is the failure of the model to simulate the recession limb of the hydrograph. The modelled recession limb falls away early consistently for all storms tested.

It was partly from considerations of the latter symptom in other circumstances (Kidd, 1972) that the non-linear reservoir surface routing submodel was postulated. It is noticeable that the non-linear submodel demonstrates a marked improvement in the simulation of the recession limb. Furthermore, the non-linear submodel consistently demonstrates an ability to simulate both the peak value and the time to peak. In general, it may be said that in all cases, the modelled output hydrograph matches closely the observed output hydrograph, and in no case is the simulation of the peak inferior to that gained by the linear submodel. From this, it is concluded that the non-linear reservoir surface routing submodel produces a good synthesis of the above-ground phase of the urban runoff process.

It may be argued that the improvement in model performance is no better than might be expected from the introduction of another degree of freedom. This argument is less valid in this case where only one value of the non-linearity parameter n (0.67) has been tried in the non-linear submodel. Furthermore, the linear submodel may be seen as a special case of the non-linear submodel, and its only advantage lies in the fact that it is simpler to program. The author considers that the advantages to be accrued from an improved synthesis outweighs the disadvantages of more complex programming. Details of the computer program used in the application of the model are given in a PhD thesis of the University of Southampton (Kidd, 1976).

Conclusions

1. The time of entry surface routing submodel does not effectively simulate the above ground phase phenomenon.

2. While synthesising the storage effects of surface routing the linear reservoir submodel does not successfully reproduce the inherent non-linearity of the above-ground phase phenomenon.

3. The non-linear reservoir surface routing submodel provides an effective simulation of the above ground phase of urban runoff.

4. The optimum values of the non-linear submodel routing constants were found to exhibit a random variation from storm to storm on a given catchment. However, the performance of the model was found to be almost as good using an overall optimum pair of parameter values as for the individual optimum pairs of values.

5. The optimum values for non-linear routing constants K_1 and K_2 were found to be 26.0 and 5.0 respectively for Lordshill catchment number 1 and 26.5 and 5.3. for Lordshill catchment number 2. The closeness of these two pair values is surprising considering the difference in average catchment slope, but it seems likely that the values might change for much flatter catchments.

Further work

This work has demonstrated the viability of the non-linear reservoir submodel as a method of synthesis of surface routing. As such, the submodel may be employed in a design sense to convert rainfall excess to inlet hydrograph. However, before it may be used in this design sense, the submodel must first be calibrated and this would seem to be the next step.

It has been shown here that the routing constants do not vary greatly between the two catchments studied; however, it seems likely that there must be some variation from catchment to catchment. Only the application of the model to a wider variety of monitored sub-catchments will provide the data from which to predict this variation. In this way the model may be calibrated by regressing the routing constants on pertinent catchment characteristics. Such a suitable data collection is in the process of being prepared, and it is hoped that suitable instrumentation will allow the runoff from subcatchments to be monitored at the phase boundary. Development of suitable instrumentation is under way at the Institute.

Looking at the urban runoff process as a whole, further work is urgently required in two other areas, the estimation of percentage runoff and below-ground routing. The first of these requires initially the collation of a large quantity of data, from which hopefully some statistical trend may become apparent between percentage runoff and pertinent physical and meteorological characteristics. Such a study is also presently being undertaken at the Institute.

The below-ground phase of the process requires further work, chiefly to establish a balance between complexity and speed in modelling the pipe routing phenomenon, as highlighted in Section II. Study is also required into junction losses and surcharging, and such work is presently being undertaken at the Hydraulics Research Station.

Work is also being done on the effects of storm movement at the Meteorological Office and at Birmingham University. If such an effect is found to be appreciable, then some reappraisal of the design storm would be necessary.

Figures 30-59 Model performance for specified storms

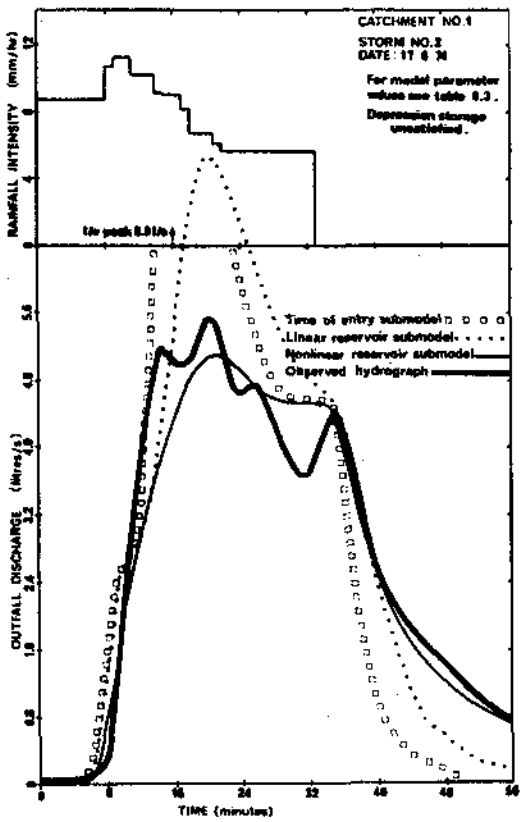

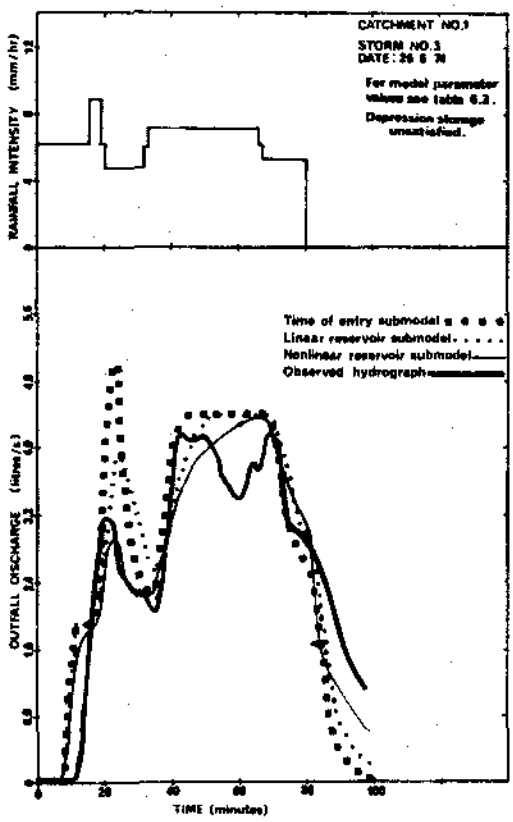

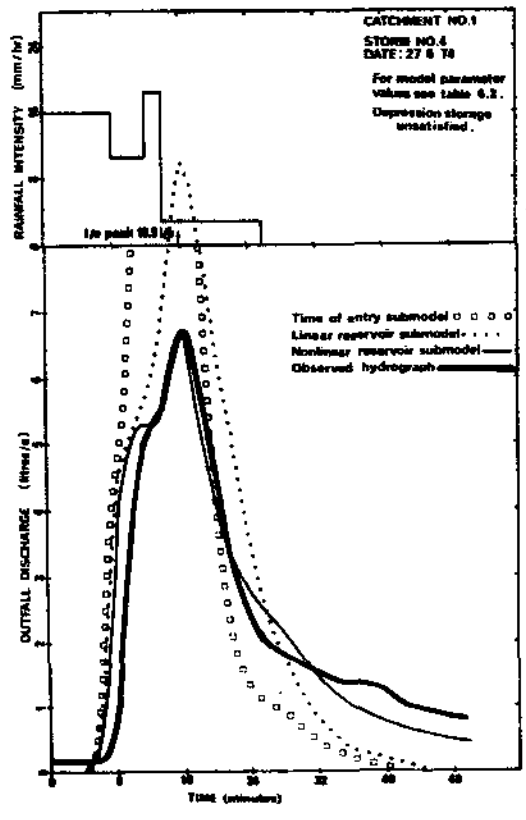

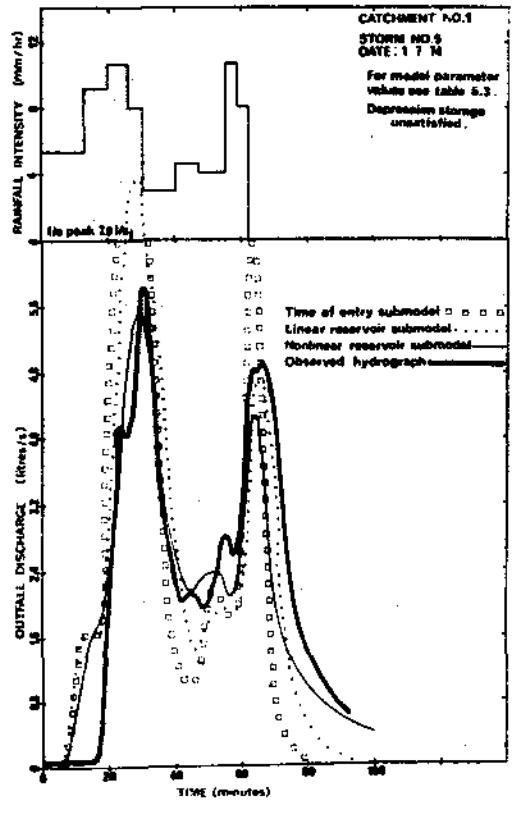

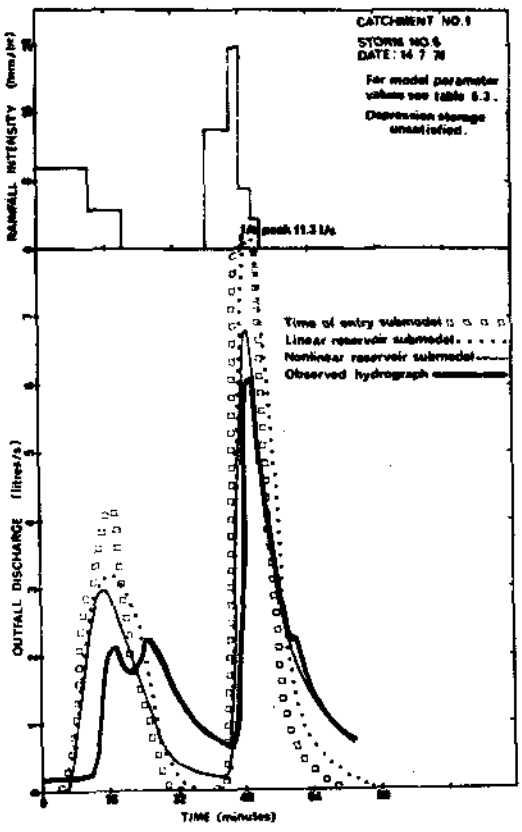
CATCHMENT NO.1
STORM NO.6
DATE : 14 7 76
For model parameter values see table 6.3.
Depression storage unsatisfied.
RAINFALL INTENSITY (mm/hr)
OUTFALL DISCHARGE (litres/s)
Time of entry submodel
Linear reservoir submodel
Nonlinear reservoir submodel
Observed hydrograph
TIME (minutes)

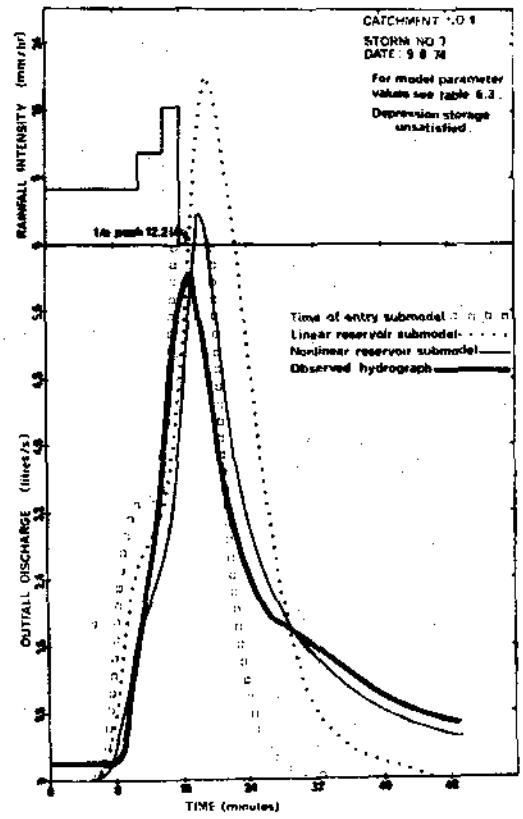
CATCHMENT NO.1
STORM NO.7
DATE : 9 8 76
For model parameter values see table 6.3.
Depression storage unsatisfied.
RAINFALL INTENSITY (mm/hr)
OUTFALL DISCHARGE (litres/s)
Time of entry submodel
Linear reservoir submodel
Nonlinear reservoir submodel
Observed hydrograph
TIME (minutes)

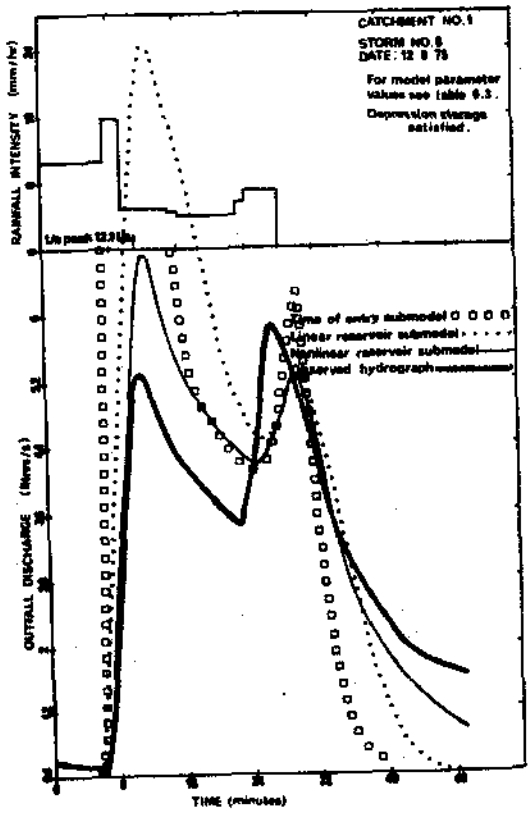
CATCHMENT NO.1
STORM NO.8
DATE : 12 8 76
For model parameter values see table 6.3.
Depression storage satisfied.
RAINFALL INTENSITY (mm/hr)
OUTFALL DISCHARGE (litres/s)
Time of entry submodel
Linear reservoir submodel
Nonlinear reservoir submodel
Observed hydrograph
TIME (minutes)

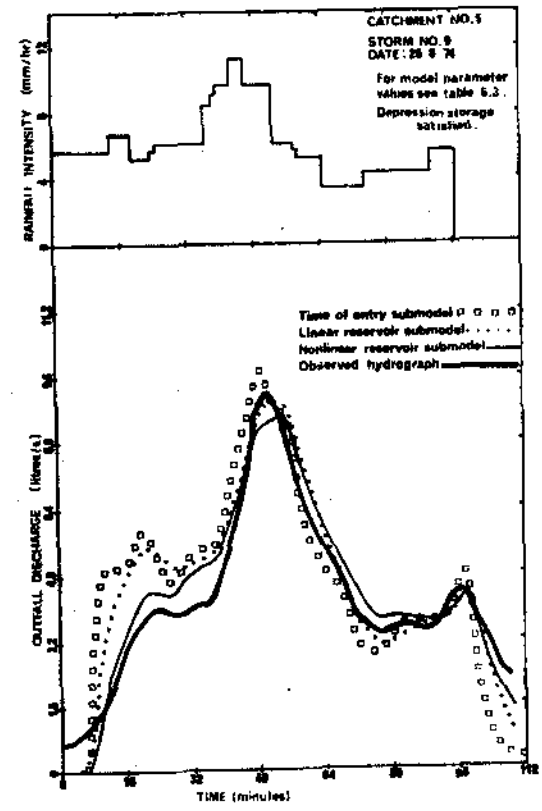
CATCHMENT NO.5
STORM NO.9
DATE : 26 8 76
For model parameter values see table 6.3.
Depression storage satisfied.
RAINFALL INTENSITY (mm/hr)
OUTFALL DISCHARGE (litres/s)
Time of entry submodel
Linear reservoir submodel
Nonlinear reservoir submodel
Observed hydrograph
TIME (minutes)

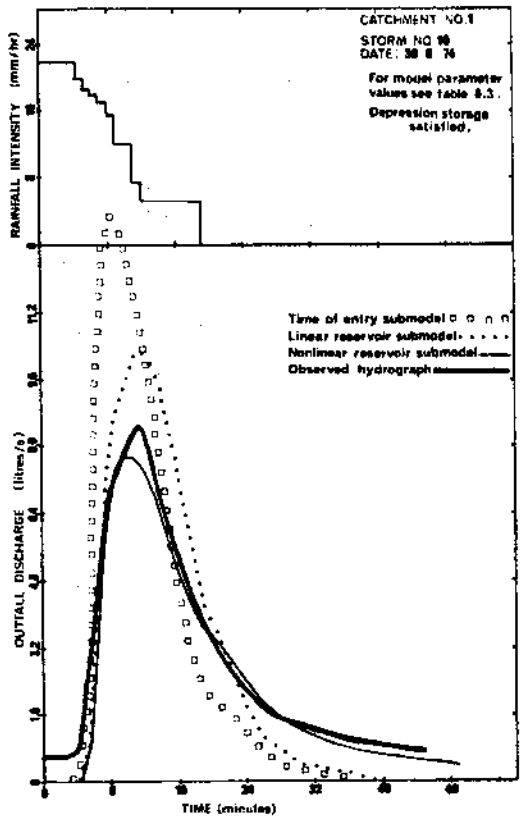
CATCHMENT NO 1
STORM NO 10
DATE : 30 8 74
For model parameter values see table 6.3.
Depression storage satisfied.
RAINFALL INTENSITY (mm/hr)
Time of entry submodel
Linear reservoir submodel
Nonlinear reservoir submodel
Observed hydrograph
OUTFALL DISCHARGE (litres/s)
TIME (minutes)

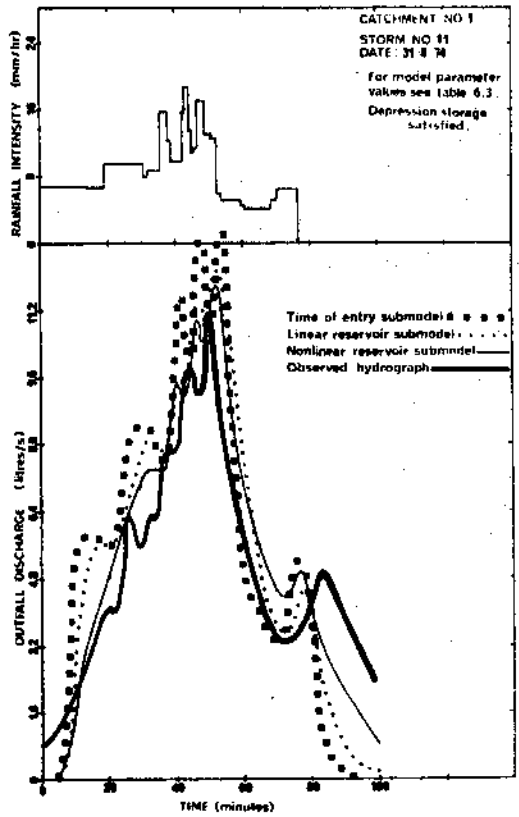
CATCHMENT NO 1
STORM NO 11
DATE : 31 8 74
For model parameter values see table 6.3.
Depression storage satisfied.
RAINFALL INTENSITY (mm/hr)
Time of entry submodel
Linear reservoir submodel
Nonlinear reservoir submodel
Observed hydrograph
OUTFALL DISCHARGE (litres/s)
TIME (minutes)

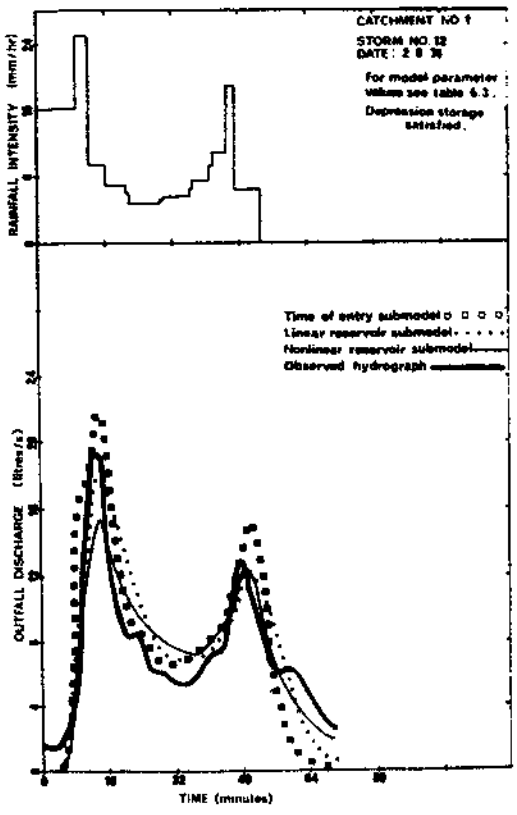
CATCHMENT NO 1
STORM NO 12
DATE : 2 9 74
For model parameter values see table 6.3.
Depression storage satisfied.
RAINFALL INTENSITY (mm/hr)
Time of entry submodel
Linear reservoir submodel
Nonlinear reservoir submodel
Observed hydrograph
OUTFALL DISCHARGE (litres/s)
TIME (minutes)

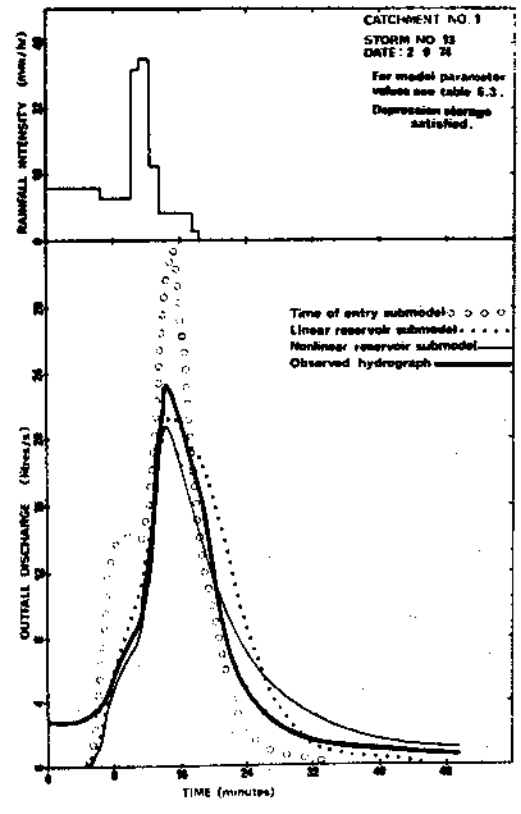
CATCHMENT NO 1
STORM NO 13
DATE : 2 9 74
For model parameter values see table 6.3.
Depression storage satisfied.
RAINFALL INTENSITY (mm/hr)
Time of entry submodel
Linear reservoir submodel
Nonlinear reservoir submodel
Observed hydrograph
OUTFALL DISCHARGE (litres/s)
TIME (minutes)

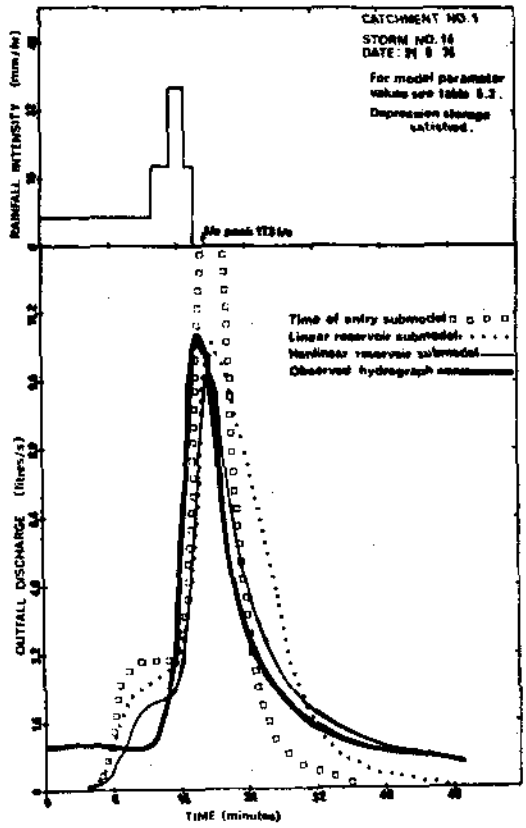
CATCHMENT NO. 1
STORM NO. 14
DATE : 21 8 74
For model parameter values see table 6.3.
Depression storage satisfied.
RAINFALL INTENSITY (mm/hr)
Time of entry submodel
Linear reservoir submodel
Nonlinear reservoir submodel
Observed hydrograph
OUTFALL DISCHARGE (litres/s)
TIME (minutes)

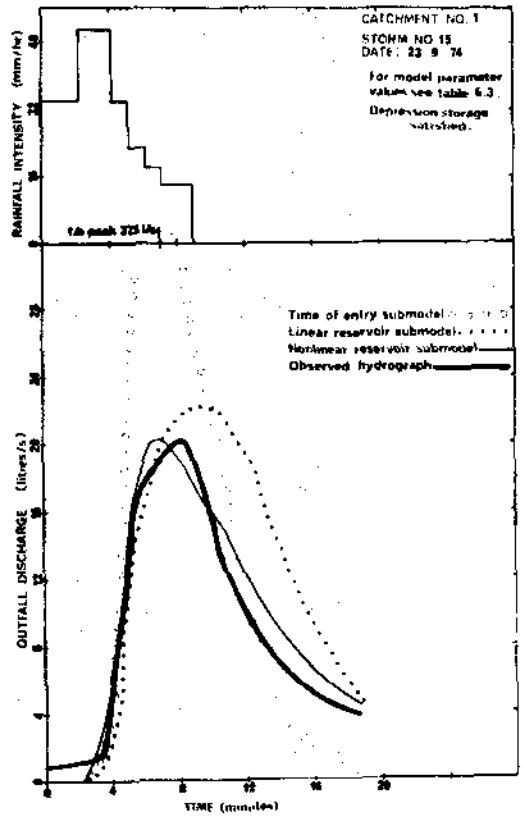
CATCHMENT NO. 1
STORM NO 15
DATE : 23 9 74
For model parameter values see table 6.3.
Depression storage satisfied.
RAINFALL INTENSITY (mm/hr)
Time of entry submodel
Linear reservoir submodel
Nonlinear reservoir submodel
Observed hydrograph
OUTFALL DISCHARGE (litres/s)
TIME (minutes)

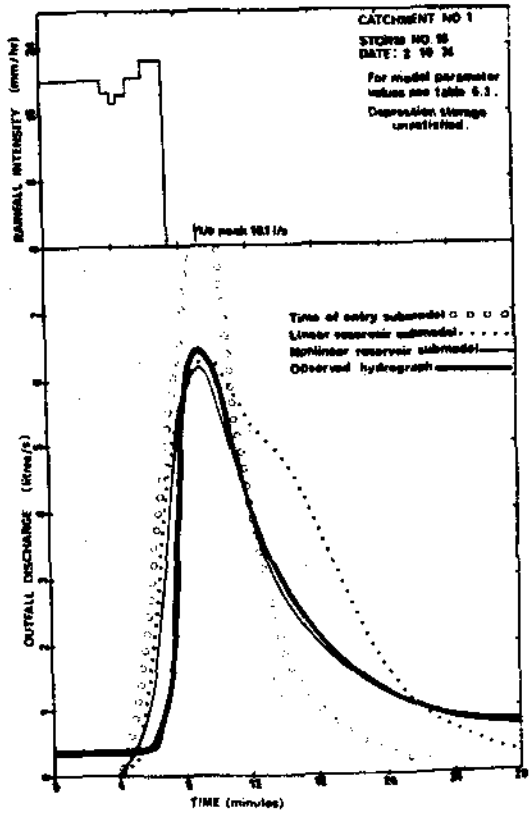
CATCHMENT NO 1
STORM NO 16
DATE : 2 10 74
For model parameter values see table 6.3.
Depression storage unsatisfied.
RAINFALL INTENSITY (mm/hr)
Time of entry submodel
Linear reservoir submodel
Nonlinear reservoir submodel
Observed hydrograph
OUTFALL DISCHARGE (litres/s)
TIME (minutes)

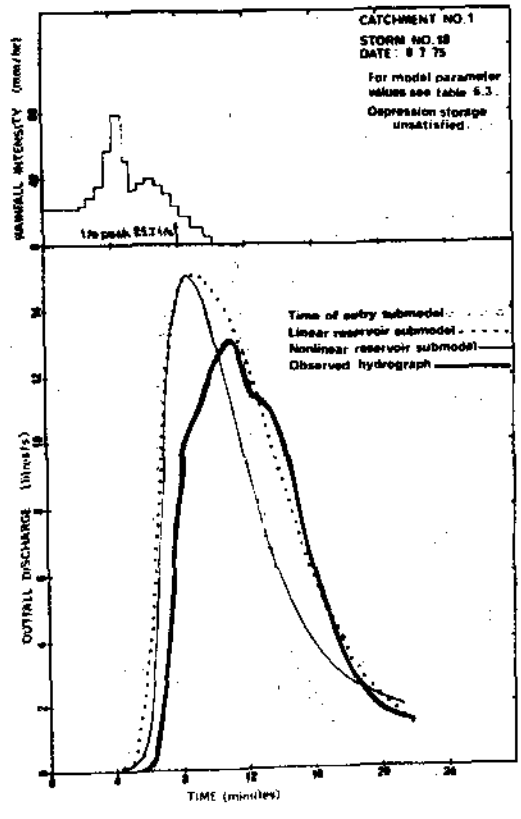
CATCHMENT NO.1
STORM NO.18
DATE : 8 7 75
For model parameter values see table 6.3.
Depression storage unsatisfied.
RAINFALL INTENSITY (mm/hr)
Time of entry submodel
Linear reservoir submodel
Nonlinear reservoir submodel
Observed hydrograph
OUTFALL DISCHARGE (litres/s)
TIME (minutes)

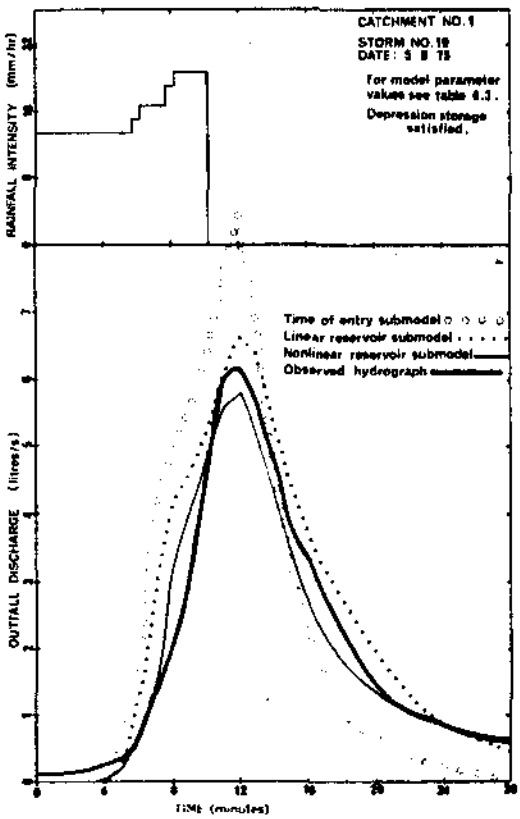
CATCHMENT NO. 1
STORM NO. 19
DATE : 5 8 75
For model parameter values see table 6.3.
Depression storage satisfied.
RAINFALL INTENSITY (mm/hr)
Time of entry submodel
Linear reservoir submodel
Nonlinear reservoir submodel
Observed hydrograph
OUTFALL DISCHARGE (litres/s)
TIME (minutes)

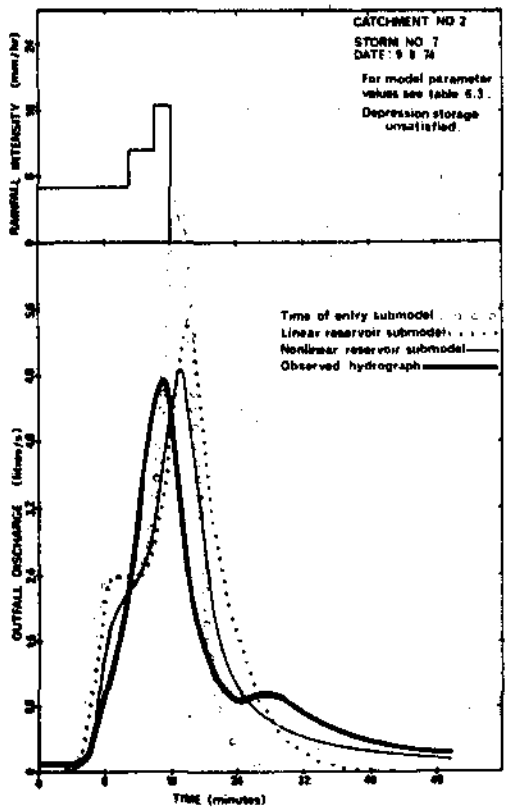
CATCHMENT NO 2
STORM NO. 7
DATE : 9 8 74
For model parameter values see table 6.3.
Depression storage unsatisfied.
RAINFALL INTENSITY (mm/hr)
Time of entry submodel
Linear reservoir submodel
Nonlinear reservoir submodel
Observed hydrograph
OUTFALL DISCHARGE (litres/s)
TIME (minutes)

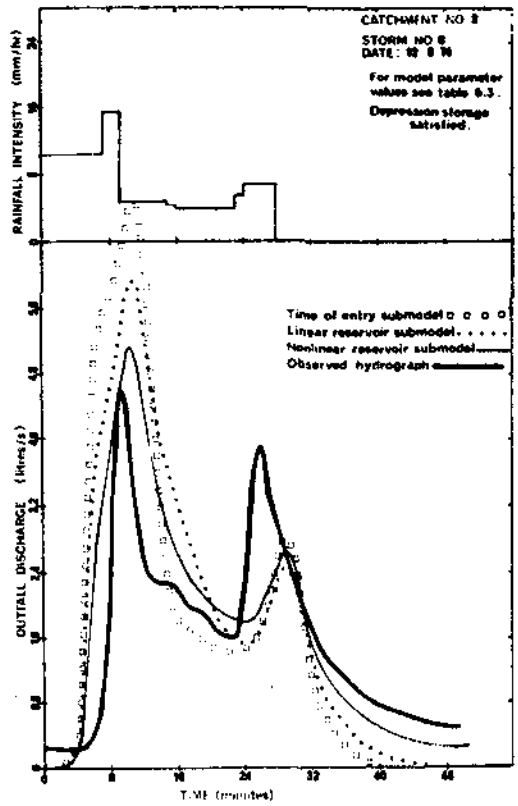
CATCHMENT NO 2
STORM NO 6
DATE : 10 8 76
For model parameter values see table 6.3.
Depression storage satisfied.
RAINFALL INTENSITY (mm/hr)
Time of entry submodel
Linear reservoir submodel
Nonlinear reservoir submodel
Observed hydrograph
OUTFALL DISCHARGE (litres/s)
TIME (minutes)

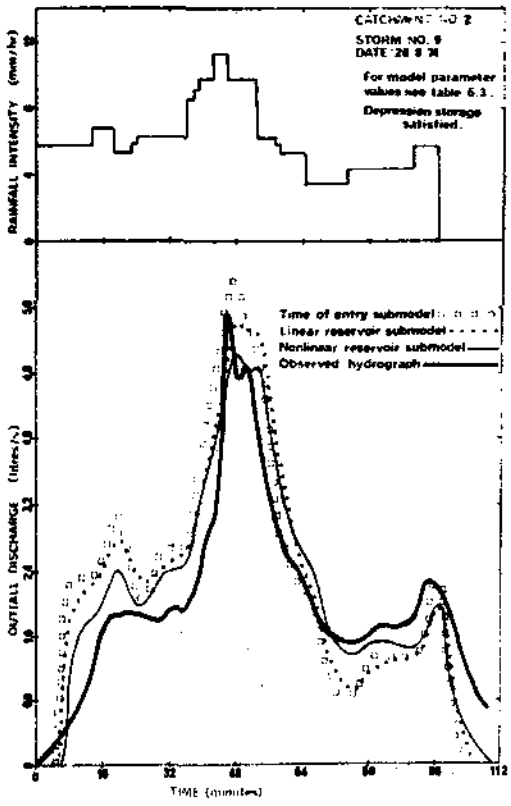
CATCHMENT NO 2
STORM NO. 9
DATE : 28 8 74
For model parameter values see table 6.3.
Depression storage satisfied.
RAINFALL INTENSITY (mm/hr)
Time of entry submodel
Linear reservoir submodel
Nonlinear reservoir submodel
Observed hydrograph
OUTFALL DISCHARGE (litres/s)
TIME (minutes)

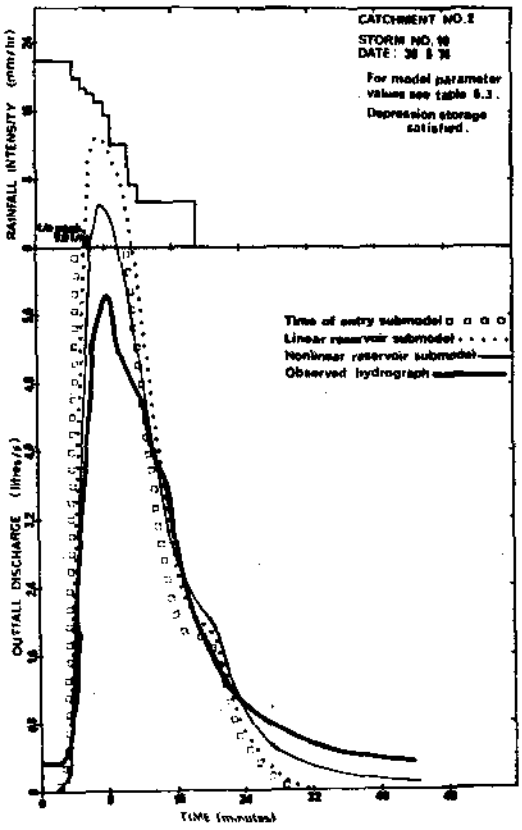
CATCHMENT NO.2
STORM NO. 10
DATE : 30 8 76
For model parameter values see table 6.3.
Depression storage satisfied.
RAINFALL INTENSITY (mm/hr)
Time of entry submodel
Linear reservoir submodel
Nonlinear reservoir submodel
Observed hydrograph
OUTFALL DISCHARGE (litres/s)
TIME (minutes)

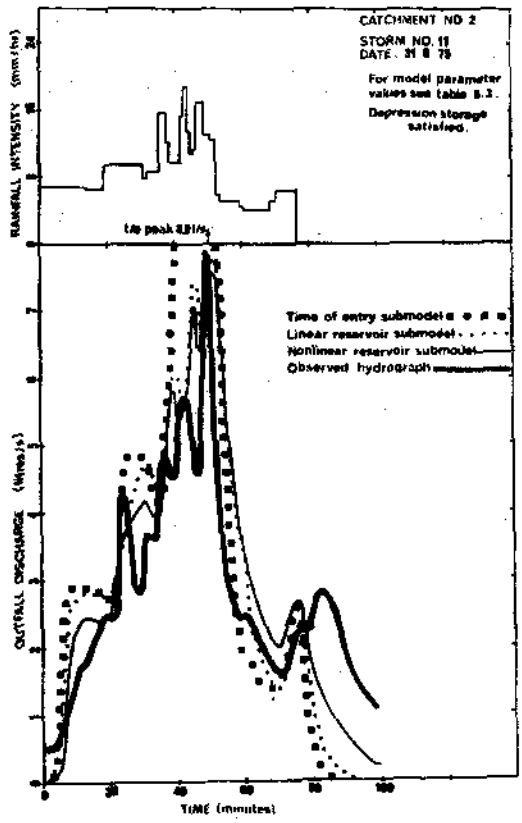
CATCHMENT NO 2
STORM NO. 11
DATE : 31 8 76
For model parameter values see table 6.3.
Depression storage satisfied.
RAINFALL INTENSITY (mm/hr)
Time of entry submodel
Linear reservoir submodel
Nonlinear reservoir submodel
Observed hydrograph
OUTFALL DISCHARGE (litres/s)
TIME (minutes)

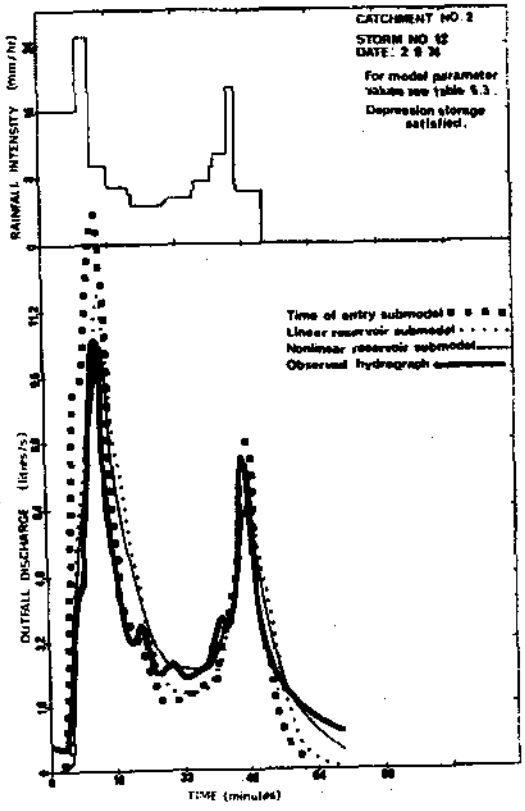
CATCHMENT NO 2
STORM NO. 12
DATE : 2 9 76
For model parameter values see table 6.3.
Depression storage satisfied.
RAINFALL INTENSITY (mm/hr)
Time of entry submodel
Linear reservoir submodel
Nonlinear reservoir submodel
Observed hydrograph
OUTFALL DISCHARGE (litres/s)
TIME (minutes)

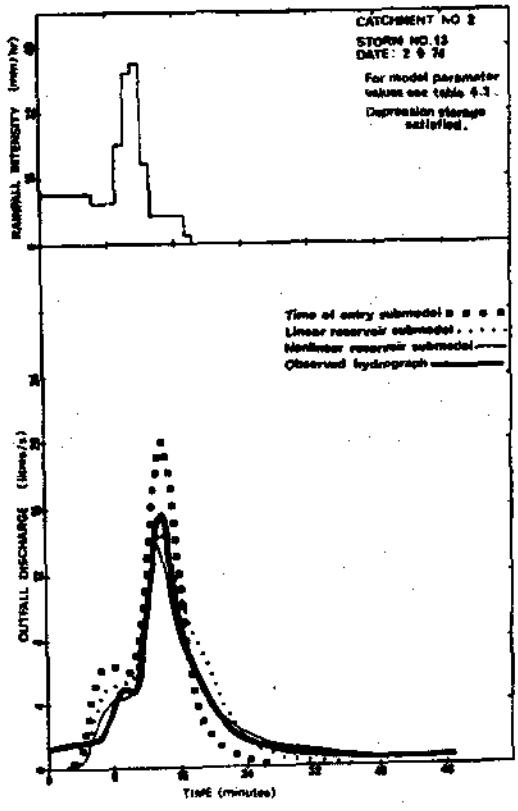
CATCHMENT NO 2
STORM NO. 13
DATE : 2 9 76
For model parameter values see table 6.3.
Depression storage satisfied.
RAINFALL INTENSITY (mm/hr)
Time of entry submodel
Linear reservoir submodel
Nonlinear reservoir submodel
Observed hydrograph
OUTFALL DISCHARGE (litres/s)
TIME (minutes)

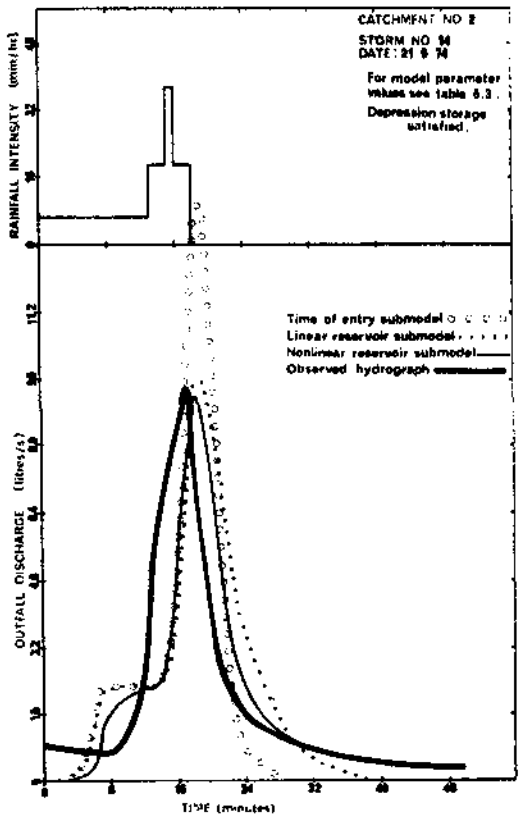
CATCHMENT NO. 2
STORM NO. 14
DATE : 21 9 74
For model parameter values see table 6.3.
Depression storage satisfied.
RAINFALL INTENSITY (mm/hr)
Time of entry submodel
Linear reservoir submodel
Nonlinear reservoir submodel
Observed hydrograph
OUTFALL DISCHARGE (litres/s)
TIME (minutes)

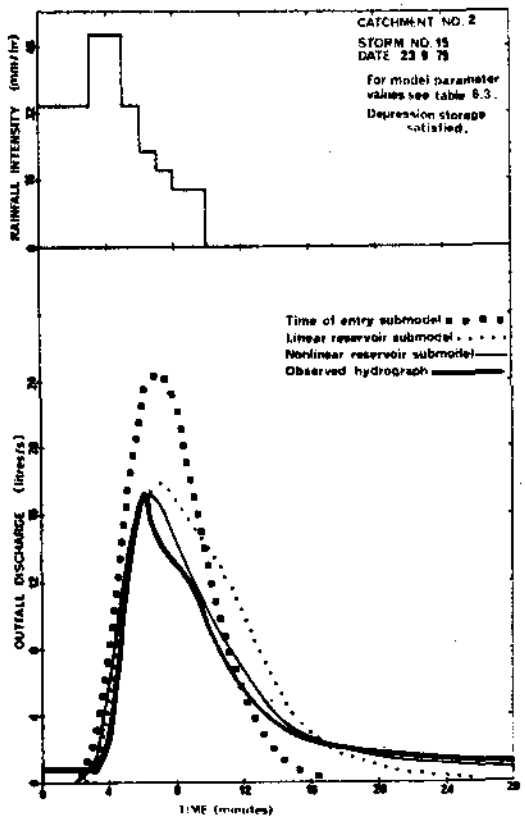
CATCHMENT NO. 2
STORM NO. 15
DATE 23 9 75
For model parameter values see table 6.3.
Depression storage satisfied.
RAINFALL INTENSITY (mm/hr)
Time of entry submodel
Linear reservoir submodel
Nonlinear reservoir submodel
Observed hydrograph
OUTFALL DISCHARGE (litres/s)
TIME (minutes)

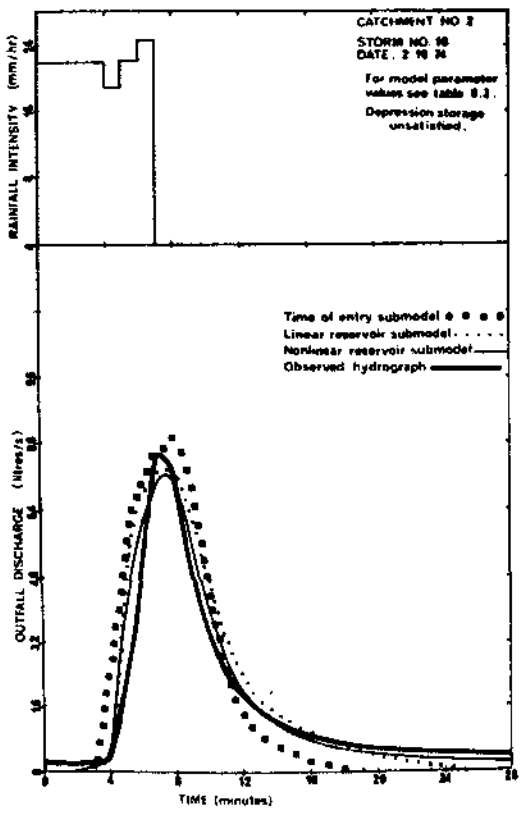
CATCHMENT NO. 2
STORM NO. 16
DATE : 2 10 74
For model parameter values see table 6.3.
Depression storage unsatisfied.
RAINFALL INTENSITY (mm/hr)
Time of entry submodel
Linear reservoir submodel
Nonlinear reservoir submodel
Observed hydrograph
OUTFALL DISCHARGE (litres/s)
TIME (minutes)

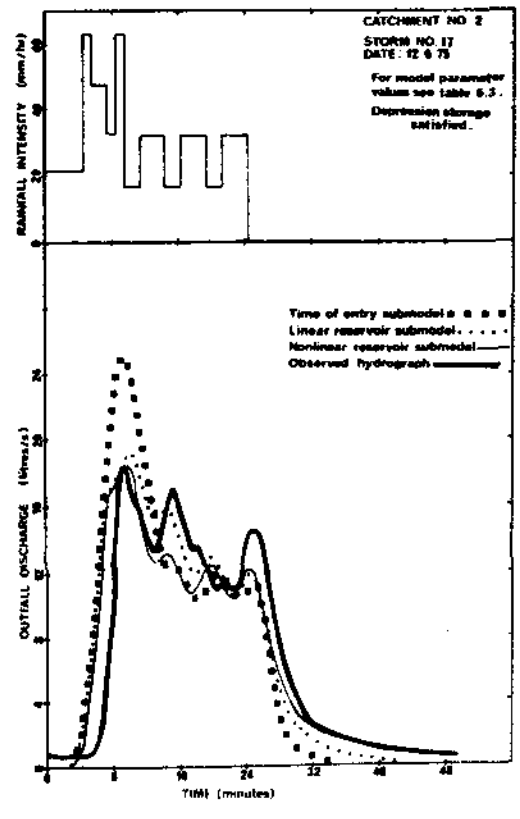
CATCHMENT NO. 2
STORM NO. 17
DATE : 12 9 75
For model parameter values see table 6.3.
Depression storage satisfied.
RAINFALL INTENSITY (mm/hr)
Time of entry submodel
Linear reservoir submodel
Nonlinear reservoir submodel
Observed hydrograph
OUTFALL DISCHARGE (litres/s)
TIME (minutes)

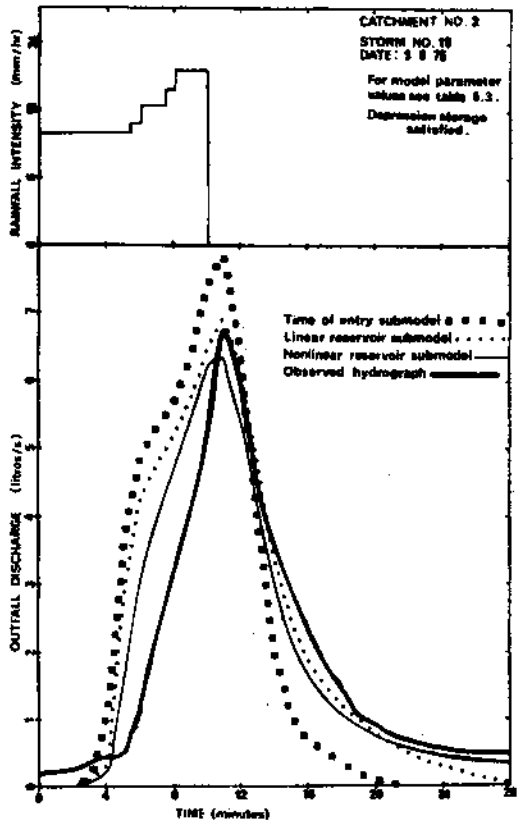
CATCHMENT NO. 2
STORM NO. 18
DATE : 5 8 75
For model parameter values see table 6.3.
Depression storage satisfied.
RAINFALL INTENSITY (mm/hr)
Time of entry submodel
Linear reservoir submodel
Nonlinear reservoir submodel
Observed hydrograph
OUTFALL DISCHARGE (litres/s)
TIME (minutes)

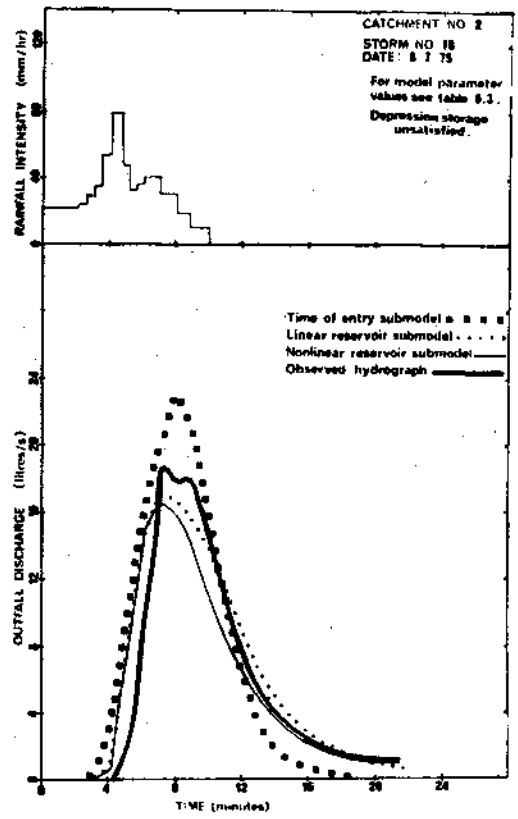
CATCHMENT NO. 2
STORM NO 15
DATE : 5 7 75
For model parameter values see table 6.3.
Depression storage unsatisfied.
RAINFALL INTENSITY (mm/hr)
Time of entry submodel
Linear reservoir submodel
Nonlinear reservoir submodel
Observed hydrograph
OUTFALL DISCHARGE (litres/s)
TIME (minutes)

REFERENCES

Abbott, M. B. 1966, "An Introduction to the Method of Characteristics". Thames and Hudson, London.

Amein, M. 1968. "An implicit method for numerical flood routing". *Wat. Resour. Res.*, *4*, (4), 719.

Bakhmeteff, B. A. 1932. "Hydraulics of Open Channels". Appendix II, McGraw-Hill, New York, 1932.

Bravo, C. A., Harley B. M., Perkins, F. E. and Eagleson, P. S. 1970. "A linear distributed model of catchment runoff". Hydro-dynamic Lab. Report No. 123, MIT.

Chow, V. T. 1959. "Open Channel Hydraulics". McGraw-Hill, New York.

Courant, R., Isaacson, E. and Rees, M. 1952. "On the solution of non-linear hyperbolic differential equations by finite differences" Communications on Pure and Applied Math., No. 5, 243.

Ding, J. Y. 1967. "Flow routing by direct integration method". International Hydrology Symposium, Fort Collins, U.S.A.

Harley, B. M., Perkins, F. E. and Eagleson, P. S. 1970. "A modular distributed model of catchment dynamics". Hydrodynamics Lab. Report No. 133, MIT.

Horner, W. W. and Flynt, F. L. 1934. "Relation between rainfall and runoff from small urban areas". *Trans. ASCE*, *60*, 1135.

Kidd, C. H. R. 1972. "The development of an urban runoff model". Unpublished M.Sc. Thesis, Queen's University, Canada.

Liggett, J. A. and Woolhiser, D. A. 1967. "Difference solutions of the shallow water equation". *Proc. ASCE. Eng. Mech. Div.*, *3*, No. EM2, 39.

Muzik, I. 1974. "Laboratory experiments with surface runoff", *Proc. ASCE, Hyd. Div.*, *100*, 501.

Price, R. K. 1974. "Comparison of four numerical methods for flood routing". *Proc. ASCE, Hyd. Div.*, *100*, 879.

Sarma, P. B. S, Delleur, J. W., and Rao, A. R. 1973. "Comparison of rainfall-runoff models for urban areas". *J. Hydrology*, *18*, 329.

Stoker, J. J. 1953. "Derivation of basic theory and formulation of numerical methods of attack". Report No. 1, "Numerical solution of flood prediction and river regulation problems", New York University Institute of Mathematical Sciences.

Tholin, A. L., and Keifer, A. M. 1960, "Hydrology of urban runoff". *Trans. ASCE*, *125*, 1308.

Veissman, W. 1966. "The hydrology of small impervious areas". *Wat. Resour. Res.*, *2*, 405.

Watkins, L. H. 1962. "The Design of Urban Sewer Systems". HMSO Road Research Laboratory Technical Paper 55.

Wooding, R. A. 1965. "A hydraulic model for the catchment stream problem". *J. Hydrology*, *3*, 254.